Journal of Medicinal Chemistry

Article

Development of blood brain barrier permeable nitrocatechol-based catechol *O*-methyltransferase inhibitors with reduced potential for hepatotoxicity

Tiago B. Silva, Tarek Mohamed, Arash Shakeri, Praveen P. N. Rao, Loreto Martínez-González, Daniel I. Pérez, Ana Martínez, Maria Joao Valente, Jorge Garrido, Eugenio Uriarte, Paula Serrão, Patricio Soares-da-Silva, Fernando Remião, and Fernanda M. Borges

J. Med. Chem., **Just Accepted Manuscript** • DOI: 10.1021/acs.jmedchem.6b00666 • Publication Date (Web): 27 Jul 2016

Just Accepted

ACS Publications

Journal of Medicinal Chemistry is published by the American Chemical Society. 1155 Sixteenth Street N.W., Washington, DC 20036

Development of blood brain barrier permeable nitrocatechol-based catechol *O*-methyltransferase inhibitors with reduced potential for hepatotoxicity

Tiago Silva[1], Tarek Mohamed[2], Arash Shakeri[2], Praveen P. N. Rao[2], Loreto Martínez-González[3] Daniel I. Pérez[3], Ana Martínez[3], Maria João Valente[4], Jorge Garrido[5], Eugenio Uriarte[6], Paula Serrão[7,8], Patrício Soares-da-Silva[7,8], Fernando Remião[4], Fernanda Borges[1*]

[1]CIQ/Department of Chemistry and Biochemistry, Faculty of Sciences, University of Porto, Rua do Campo Alegre s/n, 4169-007 Porto, Portugal

[2]School of Pharmacy, Health Sciences Campus, University of Waterloo, 200 University Avenue West, Waterloo, Ontario, Canada N2L 3G1

[3]Centro de Investigaciónes Biológicas, CSIC, C/ Ramiro de Maeztu, 28040 Madrid, Spain

[4] UCIBIO-REQUIMTE, Laboratory of Toxicology, Department of Biological Sciences, Faculty of Pharmacy, Rua de Jorge Viterbo Ferreira, 4050-313 Porto, Portugal

[5]Departamento de Engenharia Química, Instituto Superior de Engenharia do Porto (ISEP), Instituto Politécnico Porto, 4200-072 Porto, Portugal

[6] Department of Organic Chemistry, Faculty of Pharmacy, University of Santiago de Compostela, 15782 Santiago de Compostela, Spain

[7]Department of Pharmacology & Therapeutics, Faculty of Medicine, University of Porto, 4200-319 Porto, Portugal

[8]MedInUP - Center for Drug Discovery and Innovative Medicines, University of Porto, Porto, Portugal.

Corresponding Author:

Fernanda Borges, CIQUP/Department of Chemistry and Biochemistry, Faculty of Sciences, University of Porto, Porto 4169-007, Portugal. E-mail: fborges@fc.up.pt

ABSTRACT

Recent efforts have been focused on the development of centrally active COMT inhibitors, which can be valuable assets for neurological disorders such as Parkinson's disease, due to the severe hepatotoxicity risk associated with tolcapone. New nitrocatechol COMT inhibitors based on naturally-occurring caffeic acid and caffeic acid phenethyl ester were developed. All nitrocatechol derivatives displayed potent inhibition of peripheral and cerebral COMT within the nanomolar range. Drug-like derivatives **13**, **15** and **16** were predicted to cross the blood-brain barrier *in vitro* and were significantly less toxic than tolcapone and entacapone when incubated at 50 μM with rat primary hepatocytes. Moreover, their unique acidity and electrochemical properties decreased the chances of formation of reactive quinone-imines and, as such, the potential for hepatotoxicity. The binding mode of **16** confirmed that the major interactions with COMT were established via the nitrocatechol ring, allowing derivatization of the side chain for future lead optimization efforts.

Keywords: Catechol *O*-methyltransferase, caffeic acid, CAPE, nitrocatechol, hepatotoxicity

INTRODUCTION

Catechol *O*-methyltransferase (COMT, EC 2.1.1.6) catalyzes the regioselective transfer of an activated methyl group from common donor *S*-adenosyl-L-methionine (SAM) to one hydroxyl group of its catechol substrates[1], using Mg^{2+} as a co-factor and yielding a mono *O*-methylated product and *S*-adenosylhomocysteine (SAH). COMT is ubiquitously expressed and can be found mainly in the liver and kidneys, as well as within the central nervous system.[2, 3] Other peripheral sources of COMT include the lungs, stomach, spleen, intestine, heart, adrenal glands, adipose tissue, gonads, muscle and erythrocytes.[1, 4] This single domain intracellular methyltransferase is responsible for the selective *O*-methylation of endogenous neurotransmitters[5, 6], hormones[7] and xenobiotics[8] bearing a dihydroxybenzene (catecholic) scaffold. The array of xenobiotics metabolized by COMT includes dopamine precursor L-DOPA (levodopa), the gold standard drug for the clinical management of Parkinson's disease (PD)[9], which is extensively transformed to its inactive 3-*O*-methyl metabolite. Pharmacological blockade of the degradation of levodopa with COMT inhibitors prevents its peripheral degradation and increases its plasma half-life, allowing orally administered levodopa to cross the blood-brain barrier (BBB) into the brain where it is locally decarboxylated to dopamine.[10] This pharmacological approach effectively compensates the shortage of cerebral dopamine and is useful in the adjunctive therapy of PD[11], depression[12], schizophrenia[13] and other dopamine deficiency-related disorders.[14] First generation COMT inhibitors based on simple catechol scaffolds act as competitive inhibitors, but their clinical utility was hampered due to poor bioavailability.[15] COMT inhibitors with clinical relevance are depicted on Figure **1** (Compounds **1**-**4**).

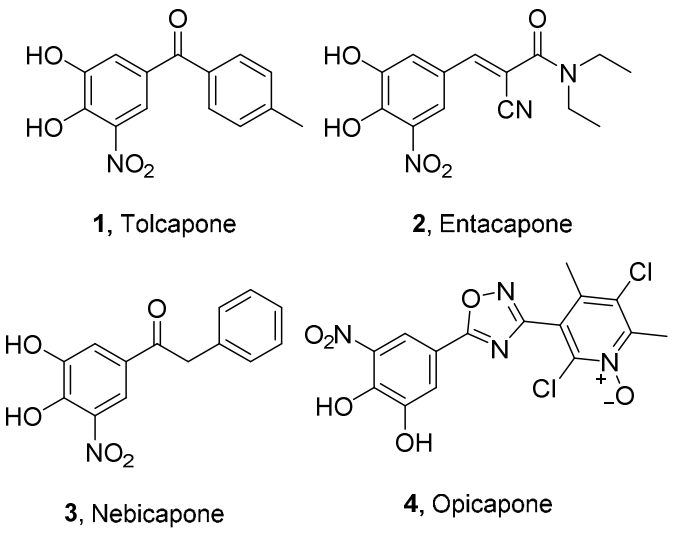

Figure 1. Chemical structures of tight-binding COMT inhibitors: tolcapone (**1**), entacapone (**2**), nebicapone (**3**) and opicapone (**4**).

Compounds **1**-**4** (Figure **1**) are structurally based on the nitrocatechol (1,2-dihydroxy-3-nitrobenzene) scaffold, the standard pharmacophore for tight binding COMT inhibitors[15], which greatly improved *in vitro* potency over competitive catechol-based inhibitors.[1, 16] Tolcapone **1** is a potent and BBB-permeable COMT inhibitor, yet its clinical use is very restricted due to its association with severe hepatotoxicity.[17] Entacapone **2** is a widely used peripheral COMT inhibitor, but its low bioavailability and short-acting inhibitory profile significantly decrease its clinical efficacy.[18] In spite of its improved pharmacokinetics, the clinical development of nebicapone **3** was discontinued because its safety profile was not considered sufficiently improved over that of tolcapone **1**.[15] Recent efforts afforded opicapone **4**, a long-acting peripheral COMT inhibitor bearing a pyridine *N*-oxide and an oxadiazole ring, which showed promising results in clinical trials[19-21] and is currently being licensed as a new treatment for PD. However, inhibition of peripheral COMT has been associated with hepatic and intestinal side effects[17, 18] and recent efforts have been focused on the development of centrally active COMT inhibitors, which can be valuable assets for neurological disorders associated with catecholamine depletion. Although encouraging results have been reported for non nitrocatechols,[15, 22-24] no significant results have been yet reported for nitrocatechol-based

derivatives. Following our line of research based on the development of new chemical entities derived from naturally-occurring scaffolds, we focused our efforts on the development of COMT inhibitors based on the hydroxycinnamic acid (HCA) (Figure **2A**) for two main reasons. Firstly, due to its privileged structure, the phenylpropanoid scaffold displays straightforward chemical diversification, which enables structural diversity and facilitates the establishment of structure-activity-property relationships. Moreover, naturally-occurring hydroxycinnamic acids like caffeic acid **5** and its derivative caffeic acid phenethyl ester (CAPE, **6**) (Figure **2A**) exhibited a wide range of biological activities[25], mainly related with neuroprotection.[26-29] Additionally, synthetic derivatives based on a similar chemical scaffold have previously been described as potent COMT inhibitors.[30] Herein, we report the synthesis, COMT inhibition, BBB permeability toxicological screening of novel HCA/nitrocatechol-based COMT inhibitors.

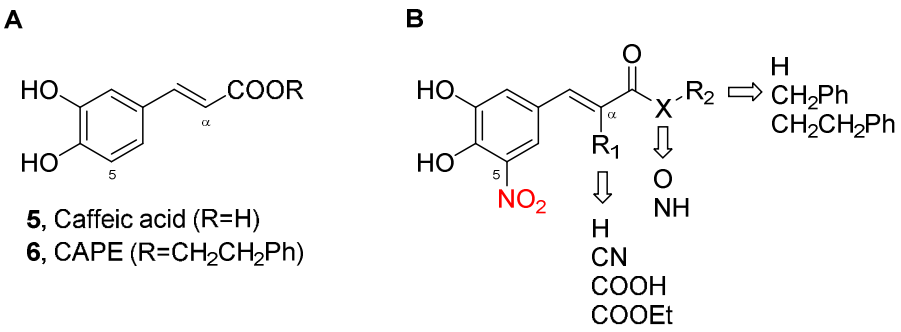

Figure 2. Chemical structures of caffeic acid and CAPE (**A**) and nitrocatechol derivatives synthesized (**B**).

RESULTS & DISCUSSION

Chemistry. A set of nitrocatechols structurally based on hydroxycinnamic acids (Figure **2B**) was obtained following the synthetic strategy depicted in Scheme **1**. Structural diversity was attained by modifying the substituents at positions C5, Cα and at the carboxylic acid function (Figure **2B**). Hydroxycinnamic derivatives containing a nitrocatechol moiety were synthetized by a Knoevenagel-Doebner condensation between 3,4-dihydroxy-5-nitrobenzaldehyde and different activated methylenes (malonic acid, cyanoacetic acid, ethyl malonate or diethyl malonate) in pyridine and catalytic amount of piperidine (step ***a***), yielding the corresponding α,β-unsaturated

derivatives **8**-**11**. Derivative **12** was obtained by alkaline hydrolysis with NaOH 2M of diester **11** in refluxing MeOH/THF. In order to derivatize the carboxylic acid group, α,β-insaturated acids **8** and **9** were then treated with the appropriate alkylaryl bromide or alkylarylamine (steps ***c*** or ***d***) to yield the corresponding esters and amides **13**-**18**. Accordingly, esters **13**-**16** were obtained by a bimolecular nucleophilic substitution between the appropriate acid (**8**-**9**) and benzylbromide or (2-bromoethyl)benzene, and amides **17** and **18** were obtained by a benzotriazol-1-yl-oxytripyrrolidinophosphonium hexafluorophosphate (PyBOP) assisted amidation between the carboxylic acid **9** and benzylamine or phenethylamine. CAPE **6** and caffeic acid benzyl ester **7** were prepared from caffeic acid **5** treated with the (2-bromoethyl)benzene or benzyl bromide (step ***c***). The structural identity and purity of all compounds was confirmed by nuclear magnetic resonance (NMR) spectroscopy (^{1}H NMR, ^{13}C NMR and DEPT135) and electronic impact mass spectrometry (EI-MS).

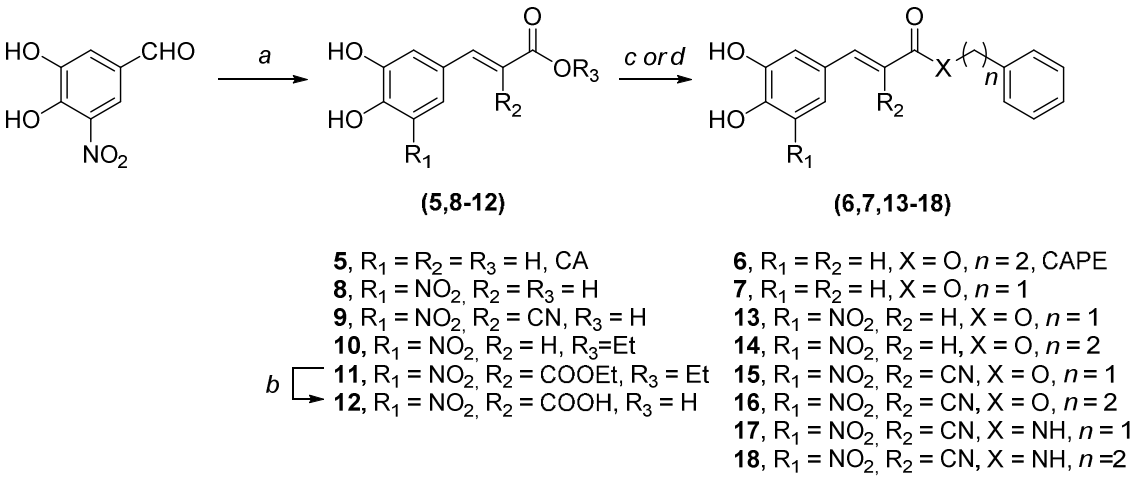

Scheme 1. Synthetic strategy pursued to obtain derivatives **8**-**18**. *a*. activated methylene, anhydrous pyridine, piperidine cat, 60°C, 7-48h; *b*. NaOH 2M, MeOH/THF, reflux, 13h; *c*. alkylarylbromide, K_3PO_4, DMSO, 0°C to rt, 24h; *d*. 1. DIPEA, DMF, PyBOP, dichloromethane, 0°C, 30'. 2. appropriate amine, rt, 6h.

Screening for COMT inhibition. In mammals, COMT is present in two forms: a soluble cytosolic form (S-COMT) and a membrane-bound form (MB-COMT). Although none of the isoforms is tissue-specific[3], S-COMT is found mainly in peripheral tissues (particularly in the

liver) and MB-COMT occurs predominantly in the brain.[31] These isoenzymes share the same primary aminoacid sequence at the catalytic site but show a different kinetic behavior, with MB-COMT showing higher substrate affinity (lower K_M) and S-COMT displaying higher capacity (higher V_{max}).[32] Hence, MB-COMT is responsible for the regulation of low physiological levels of catecholamine neurotransmitters (*e.g.* dopamine, norepinephrine and epinephrine) within the central nervous system (CNS) and, upon a sudden increase of catechol substrates (*e.g.* xenobiotic catechols), S-COMT steps up when a higher metabolic rate is required.[33, 34] Accordingly, the *in vitro* COMT inhibitory activity of the compounds under study was evaluated in rat liver and brain homogenates by measuring the formation of metanephrine (*O*-methylated adrenaline), as previously described.[35] The results, expressed as IC_{50} ± S.E.M. (n = 4 to 10), are shown in Table **1** and Figure **S2** (*Supplementary information*).

Table 1. *In vitro* COMT inhibition obtained for compounds **5**-**18** and standard inhibitors tolcapone (**1**) and entacapone (**2**).

Entry	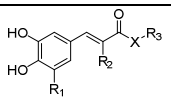				***IC_{50} (95% C.I.), nM***		***Liver/Brain ratio[a]***
	R_1	***R_2***	***R_3***	***X***	***Rat liver COMT***	***Rat brain COMT***	
5	H	H	H	O	5861	92.82 (44.98, 191.50)	63.14
6	H	H		O	*b*	*b*	-
7	H	H		O	*b*	*b*	-
8	NO_2	H	H	O	12.84 ± 0.54	5.79 ± 0.34	2.22
9	NO_2	CN	H	O	55.35 ± 15.37	100.71 ± 18.25	0.55
10	NO_2	H	Et	O	11.35 ± 0.25	1.64 ± 0.05	6.93
11	NO_2	COOEt	Et	O	12.82 ± 1.02	0.84 ± 0.02	15.23
12	NO_2	COOH	H	O	329.34 ± 75.68	180.39 ± 68.54	1.83
13	NO_2	H		O	52.47 ± 8.54	1.92 ± 0.28	27.39
14	NO_2	H		O	124.87 ± 2.72	5.02 ± 0.48	24.90

15	NO_2	CN		O	137.60 ± 11.24	4.78 ± 0.12	28.82
16	NO_2	CN		O	64.81 ± 15.84	3. 77 ± 0.51	17.18
17	NO_2	CN		NH	29.86 ± 2.35	3.14 ± 0.32	9.52
18	NO_2	CN		NH	54.85 ± 11.96	5.56 ± 1.07	9.86
1	-	-	-	-	30.59 ± 4.85	0.91 ± 0.17	33.62
2	-	-	-	-	34.45 ± 9.01	3.47 ± 0.48	9.93

Results are expressed as mean IC_{50} ± S.E.M. (n = 4 to 10). [a] IC_{50} (Liver)/IC_{50} (Brain), [b] Inactive.

Results show that compounds **5**-**7**, lacking the 5-nitro group, display weak or no inhibitory activity towards both isoforms, which is in accordance with previous reports[1, 36]. On the contrary, all derivatives bearing a 5-nitro substituent **8**-**18** were active within the nanomolar range against both isoforms. This finding stresses the utmost importance of the presence of a 5-nitro group for COMT inhibition. Moreover, and with the exception of **9**, all compounds showed higher potency towards the cerebral enzyme, which reflects the higher affinity of MB-COMT towards these compounds. Generally, the introduction of bulky groups (benzyl, phenethyl) on the carboxylic acid decreased the potency towards hepatic COMT, but the same observation did not apply for the cerebral isoform (see **8** *vs* **13**-**14**, Table **1**). Similarly, the introduction of nitrile substituent (**8** *vs* **9**) resulted in a ~3-fold decrease in inhibitory potency towards hepatic COMT, which was even more marked in the cerebral isoform (~15-fold). However, and contrarily to what was observed for the hepatic enzyme, the introduction of bulky benzyl and phenethyl groups restored the inhibitory potency towards brain COMT (**9** *vs* **15**-**18**). Ethyl ester **10** and diethyl ester **11** showed remarkable inhibitory potency towards the two isoforms, comparable to that of standard inhibitor tolcapone **1**. Interestingly, the potency of **11** showed a 20-fold (liver) and 130-fold (brain) potency decrease when the ethyl ester moieties were hydrolyzed to the corresponding carboxylic acids (compound **12**). Finally, albeit the substitution of the carboxylic ester **15** for an amide function **17** restored peripheral COMT

inhibition, it had no significant effect in the case of *N*-phenethylamide derivative **18**. Generally, and with the exception of compounds **11** and **12**, the pharmacological profile obtained for the test compounds was similar to that observed for entacapone **2**.

Evaluation of in vitro BBB permeability and drug-like properties. One of the main obstacles in drug development for CNS diseases is the drug's penetration across the BBB at therapeutic concentrations. The BBB is a complex interface between blood and the CNS that strictly controls the exchanges between the blood and brain compartments.[37] This barrier is composed of endothelial cells with tight junctions that protect the brain from potentially damaging materials.[38] The majority of CNS drugs enter the brain by transcellular passive diffusion, due to the presence of tight junction structure and limited transport pathways. Parallel artificial membrane permeability assay (PAMPA) is a high throughput technique developed to predict passive permeability through biological membranes. In order to explore the capacity of **5**-**18** compounds to penetrate into the brain, the PAMPA-BBB method described by Di *et al.*[39] was used. The *in vitro* permeabilities (*Pe*) of commercial drugs through a porcine brain lipid membrane extract, together with compounds **5**-**18**, were determined and are described in Table **2**. An assay validation was made comparing the reported permeability values of commercial drugs with the experimental data obtained. A good correlation between experimentally and described values was obtained *Pe* (exptl)= 1,1534(bibl) - 0.9936 (R^2= 0.984) (Figure **S3**, *supplementary information*). From this equation, and following the pattern established in the literature for BBB permeation prediction[40], the compounds were classified as (*a*) compounds with high BBB permeation (CNS+): $Pe > 3.62 \times 10^{-6}$ cm·s^{-1}, (*b*) compounds with low BBB permeation (CNS−): $Pe < 1.31 \times 10^{-6}$ cm·s^{-1} and (*c*) compounds of uncertain BBB permeation (CNS±): 1.31×10^{-6} cm·s^{-1} < Pe < 3.62×10^{-6} cm·s^{-1}. Based on these results, compounds **6**, **7**, **13** and **14** are predicted to be able to cross the BBB by passive permeation. Moreover, **15** and **16** showed a permeability behaviour similar to that observed for tolcapone, a well-established BBB

permeable drug with CNS activity.[41,42] Additionally, the results obtained for entacapone **2** were in accordance with its peripheral pharmacological activity[18].

Table 2. Permeability (*Pe*, 10^{-6} cm·s^{-1}) for compounds **5-18** with their predictive penetration in the CNS in the PAMPA-BBB assay.[a]

Entry	*Pe* (10^{-6}cm·s^{-1}) ± S.D.	*Prediction*
5	-	CNS - [41]
6	6.1 ± 0.4	CNS +
7	6.2 ± 0.8	CNS +
8	0.6 ± 0.4	CNS -
9	0.3 ± 0.1	CNS -
10	1.0 ± 0.1	CNS -
11	0.6 ± 0.1	CNS -
12	0.4 ± 0.3	CNS -
13	4.8 ± 0.1	CNS +
14	5.0 ± 0.1	CNS +
15	2.6 ± 0.1	CNS ±
16	2.7 ± 0.9	CNS ±
17	0.6 ± 0.1	CNS -
18	1.2 ± 0.1	CNS -
1	1.5 ± 0.1	CNS ±
2	0.3 ± 0.6	CNS -

[a]PBS:EtOH (70:30) was used as solvent; [b]Data are the mean ± S.D. of two independent experiments. CNS+: compounds with high BBB permeation; CNS±:compounds with uncertain BBB permeation; CNS−: compounds of low BBB permeation

In early drug discovery, the evaluation of absorption, distribution, metabolism, excretion and transport (ADMET) properties is of crucial importance to reduce late attrition in the development process. To further characterize the drug-likeness of the most promising CNS+/CNS± compounds **13**-**16**, several physicochemical parameters were calculated, including lipophilicity (clogP), topological polar surface area (tPSA), molecular weight (MW), ligand efficiency (LE), ligand-lipophilicity efficiency (LLE)[44] and ligand-efficiency-dependent lipophilicity (LELP)[45] for the cerebral COMT isoform. These parameters were compared to the standard COMT inhibitors tolcapone **1** and entacapone **2** (Table **3**). The clogP value was in all cases lower than 5, which is in agreement with the general requirements for drug-likeness, and within the optimal range for orally administered drugs (clogP ~3).[46,47] Additionally, the MW falls within the scope for optimal bioavailability (MW < 400 $gmol^{-1}$).[48] Moreover, the estimated tPSA values were in the same range of those obtained for tolcapone (**1**) and entacapone (**2**).[48]

Table 3. Drug-likeness of compounds **13**-**16** and standard COMT inhibitors tolcapone **1** and entacapone **2**[a]

Entry	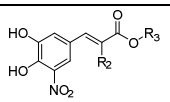		*MW* ($gmol^{-1}$)	*pIC$_{50}$*[b]	*clogP*[c]	*tPSA* ($Å^2$)[d]	*LE*[e]	*LLE*[f]	*LELP*[g]
	R2	*R3*							
13	H		315,28	8.73	3.27	112.58	0.53	5.46	6.15
14	H		329,31	8.31	3.48	112.58	0.48	4.83	7.18
15	CN		340,29	8.32	2.99	136.38	0.47	5.33	6.42
16	CN		354,32	8.43	3.20	136.38	0.45	5.23	7.04
1	-	-	273,24	9.04	2.99	103.35	0.63	6.05	4.73
2	-	-	305,29	8.52	1.64	130.38	0.54	6.98	3.02

[a] Properties determined using Molinspiration Cheminformatics software®; [b] $pIC_{50} = -\log[IC_{50}(\text{brain, mol/L})]$; [c] Partition coefficient; [d] Topological polar surface area; [e] $LE = -1.4(\log[IC_{50}(\text{brain, mol/L}) / \text{number of heavy atoms}$; [f] $LLE = pIC_{50} - \text{clogP}$; [g] $LELP = \text{clogP} / LE$.

To evaluate the lipophilicity and structural contributions to *in vitro* potency[46], LE, LLE and LELP were calculated using the pIC_{50} from rat brain COMT inhibition data (Table **3**). With the exception of **14**, the LLE was above 5, which is a value suitable for drug candidates.[46] Derivatives **13-16** complied with the recommendations of Keserü and Makara for good hits and leads[45], with LE > 0.40–0.45 and LELP between 0 and 7.5. To further characterize the relationship between lipophilicity and potency, clogP *vs* pIC_{50} values were plotted for compounds **13-16** and standard inhibitors tolcapone **1** and entacapone **2** (Figure **3**). All compounds displayed acceptable cLogP values within the preferred range for CNS drugs of 2−4 (green dotted lines, Figure **3**).[49] Compounds **13**, **15** and **16** combined optimal lipophilicity and the appropriate LLE profile (grey highlighted area) to meet the requirements for CNS drugs (Figure **3**). Potent and ligand efficient COMT inhibitors with moderate lipophilicity were thus prepared in the current series, showing an improvement in LE optimization compared to recently reported N-heterocyclic pyridinone-based COMT inhibitors.[24] Overall, these compounds showed the appropriate properties to be considered as CNS leads.

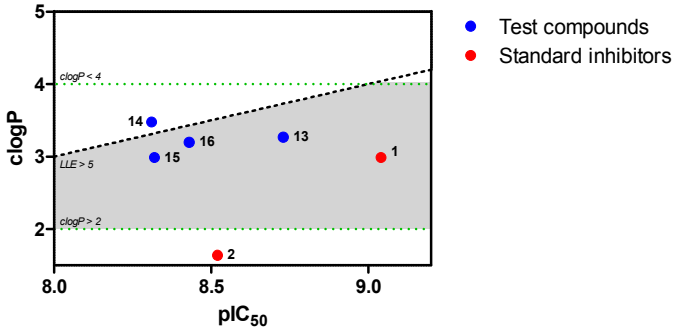

Figure 3. Distribution of clogP versus pIC_{50} values for **13-16** (blue dots) and standard inhibitors tolcapone **1** and entacapone **2** (red dots). The green dotted lines represent the preferred range for cLogP values and the black dashed line indicates the lower LLE limit for oral bioavailability. The grey highlighted area shows the area that meets optimal lipophilicity and LLE requirements for CNS drugs.

Hepatotoxicity screening of the most promising compounds. To address the risk of hepatotoxicity and evaluate the safety of the most promising compounds, cellular viability assays were run in primary rat hepatocytes incubated for 24h with three different concentrations (1, 10 and 50 μM) of compounds **13**, **15** and **16** and compared to the behavior of standard inhibitors tolcapone **1** and entacapone **2**. Cellular viability was evaluated by two methods, the methylthiazolyldiphenyl-tetrazolium bromide (MTT) reduction assay, which estimates mitochondrial function[50] and the neutral red (NR) uptake assay, which is a direct measure of cellular viability.[51] The results are expressed as mean MTT reduction (% of control) ± S.D. and NR uptake (% of control) ± S.D. (n = 4) and are depicted in Figure **4**.

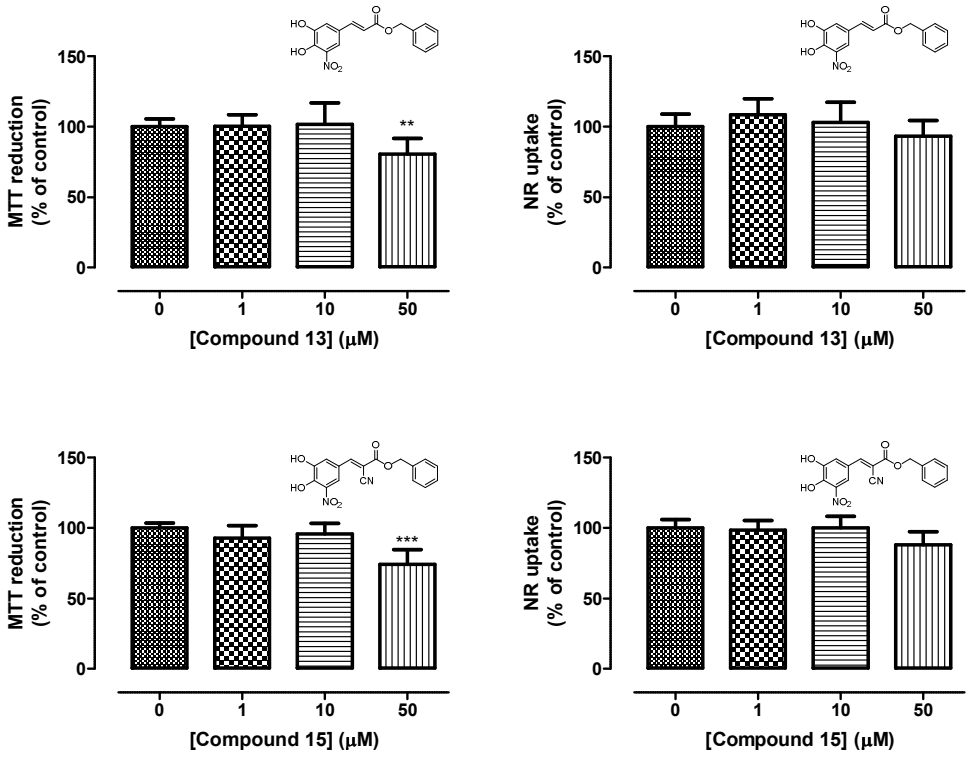

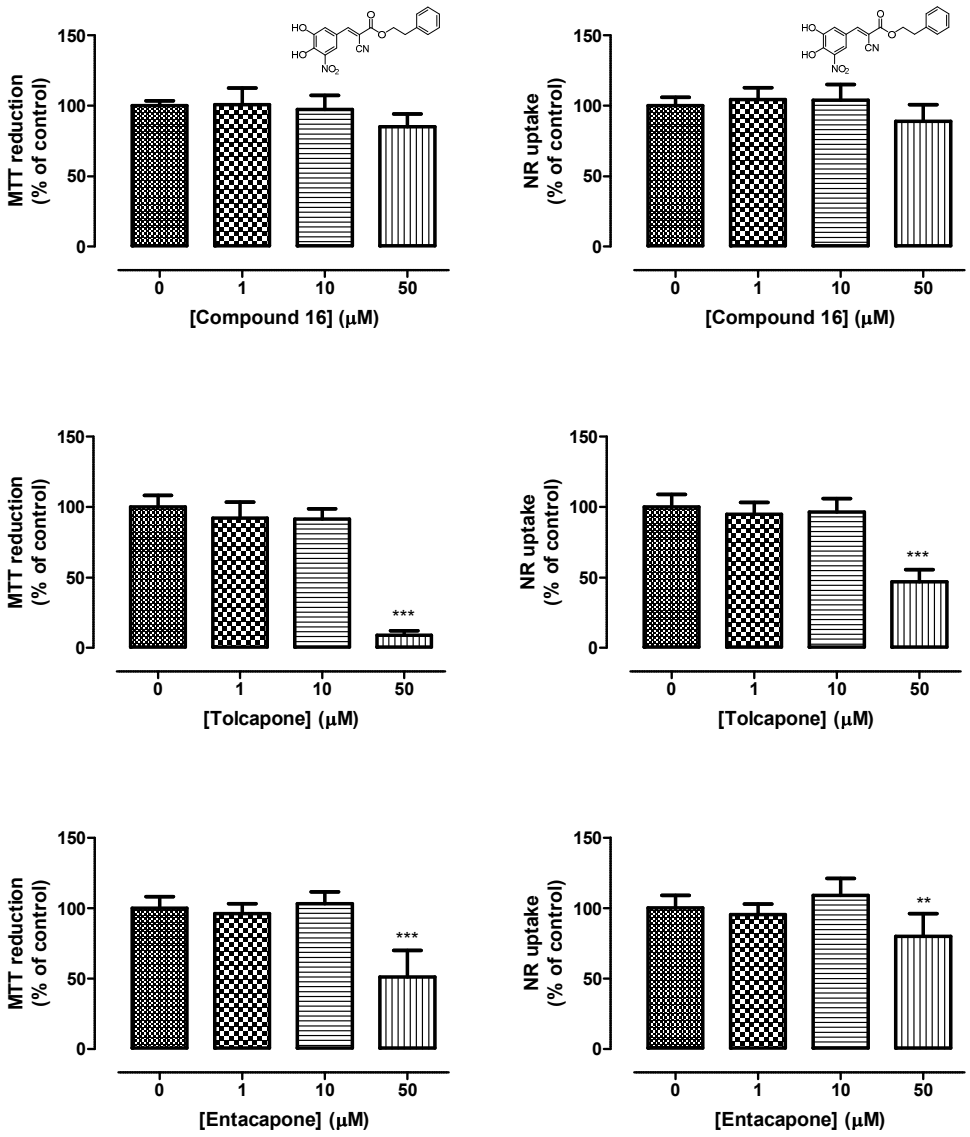

Figure 4. Cellular viability of primary rat hepatocytes after a 24h treatment with three different concentrations (1, 10 and 50 μM) of compounds **13**, **15**, **16** and standard inhibitors tolcapone **1** and entacapone **2**. Cellular viability was evaluated using two methods: MTT reduction (left) and NR uptake (right). Results are expressed as mean % of untreated controls ± S.D. (n = 4).

The results obtained show that significant reductions in cellular viability (≤ 85 % viability or ≥ 15 % of cell death) were only observed for compounds **13** (% MTT reduction = 80.69 ± 10.90, $p < 0.01$) and **15** (% MTT reduction = 74.93 ± 10.62 $p < 0.001$) at the highest concentration (50 μM), with no significant reductions on NR uptake at all concentrations. These effects were mild when compared to those observed for entacapone **2** (% MTT reduction =

51.17 ± 18.87, $p < 0.001$ and % NR uptake= 79.89 ± 16.31, $p < 0.01$) and especially tolcapone **1** which induced a massive loss of cellular viability at the highest concentration (% MTT reduction = 9.096 ± 3.263, $p < 0.001$ and % NR uptake = 46.86 ± 8.639, $p < 0.001$). Compound **16** did not induced any significant cytotoxic effect at all concentrations for both viability endpoints (% MTT reduction = 85.05 ± 9.12 and % NR uptake = 88.75 ± 12.08), indicating a noticeable improvement in the safety range when compared to tolcapone **1** and entacapone **2**.

The mild to absent cytotoxicity of the selected compounds at high micromolar concentrations in rat primary hepatocytes and, mainly, the notoriously different toxicological behavior of tolcapone gave rise to the following enquiry: how can compounds bearing the same toxicophore (nitrocatechol moiety) display such different safety profiles? The fact that the most pronounced effect was observed in the MTT assay suggests that cytotoxicity is triggered by mitochondrial toxicity. This observation is in accordance with the hypothesis that nitrocatechols and, especially, tolcapone hinder mitochondrial function through uncoupling of the respiratory chain.[52] Our results show that the toxic effects may be subverted by modulation of the chemical structure while maintaining the nitrocatechol scaffold, the toxicophore responsible for the formation of reactive and toxic intermediates.[53]

Electrochemical studies and redox behavior. Considering the presence of a catechol moiety in all the tested compounds, it was hypothesized that a redox cycling mechanism could be potential cytotoxicity trigger. Under aerobic conditions, catechols undergo auto or enzymatic-catalyzed oxidation to generate highly reactive quinones, which can impair proteins by forming sulfhydryl adducts or lead to GSH depletion. In this process, high amounts of reactive oxygen and nitrogen species are produced, which triggers oxidative stress and leads to mitochondrial dysfunction. Indeed, redox cycling compounds can induce uncoupling of the mitochondrial electron transport chain and trigger cytotoxic mechanisms that ultimately culminate in cell death.[54] In order to characterize the potential for redox cycling, we performed electrochemical studies to evaluate the redox behavior of the nitrocatechol derivatives **13**-**16** and standard

inhibitors tolcapone **1** and entacapone **2.** Electrochemical evaluation was performed at physiological pH 7.4 by differential pulse (DPV) and cyclic voltammetry (CV), using a glassy carbon working electrode, and the results are depicted on Table **4**. The oxidative behaviour was studied using DPV over the interval 0.0 V and + 0.60 V. Tolcapone **1** and entacapone **2** presented the higher oxidation potential (E_{ap}) values. In all cases, one well-defined anodic peak over the entire pH range examined was observed (Figure **5A**). The observed waves are related to the oxidation of the catechol group present in the structure of these molecules. The anodic peak potential was shifted to more negative values on increasing the solution pH. The Ep–pH plots show that the electrode process is pH-dependent (data not shown). From these plots, pKa values of 4.3 and 7.4 were inferred for tolcapone and compound **16**, respectively. These results designate a striking difference in the acidity of clinical COMT inhibitors and the new derivatives described in this report.

Table 4. Electrochemical behaviour and redox potentials of compounds 13-16, tolcapone and entacapone.

Entry	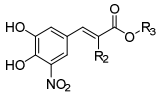		E_{ap} (mV) oxidation	Oxidation mechanism	E_{cp} (mV) reduction	Reduction mechanism
	R_2	R_3				
13	H		218	Irreversible	−616	Irreversible
14	H		217	Irreversible	−617	Irreversible
15	CN		219	Irreversible	−608	Irreversible
16	CN		275	Irreversible	−615	Irreversible
1	-	-	337	Irreversible	−671	Irreversible
2	-	-	325	Irreversible	−667	Irreversible

CV experiments showed a single oxidation peak for compounds **13-16**, tolcapone and entacapone without any distinct reduction wave on the reverse sweep, indicating an irreversible oxidation mechanism (Figure **5B**). In contrast, the CV data obtained for CAPE **6** was characteristic of an electrochemical reversible reaction, showing one anodic peak and one

cathodic peak on the reverse scan, This electrochemical behavior corresponds to the reversible formation of the corresponding *o*-quinone, and is characteristic of catechols.[55] An integrated analysis of the all CV experiments shows that the electrochemical behavior observed for compounds **13**-**16**, tolcapone **1** and entacapone **2** was not consistent with the formation of *o*-quinones. The observed modification in the oxidative behavior is undoubtedly due to the presence of the strong electron-withdrawing 5-nitro group in the test compounds and standard inhibitors. The results suggest that the electrochemically generated nitro-*o*-quinone is unstable in the time scale of the CV experiment. These findings are consistent with the data found in literature for nitrocatechol oxidation.[56] Generally, the E_{ap} values for derivatives **13**-**16** were within the same range, with the α-nitrile derivative **16** showing a slight increase in the oxidation potentials (~ 60 mV) when compared to its non-substituted analogue. Accordingly, the toxic effects observed in the experiments with primary rat hepatocytes cannot be due to redox cycling and oxidative stress induced by catechol oxidation and *o*-quinone formation.

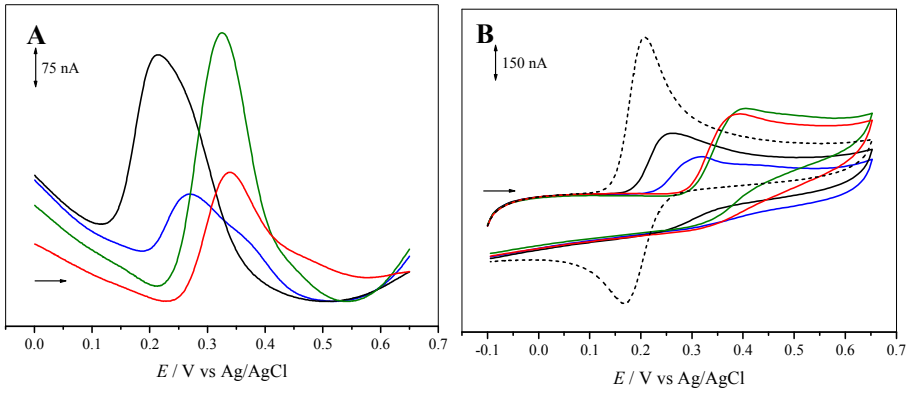

Figure 5. (A) Differential pulse voltammograms for 0.1 mM solutions of (—) tolcapone, (—) entacapone, (—) 14 and (—) 16, in physiological pH 7.4 supporting electrolyte. Scan rate: 5 mV s^{-1}; **(B)** Cyclic voltammograms for 0.1 mM solutions of (—) tolcapone, (—) entacapone, (—) 14, (—) 16 and (▪▪▪) CAPE, in physiological pH 7.4 supporting electrolyte. Scan rate: 20 mV s^{-1}

Since oxidation was mechanistically ruled out as a cytotoxic trigger, we then studied the reductive behavior of the test compounds and standard inhibitors. It has been previously suggested that the mechanism of tolcapone-induced hepatotoxicity involved the reduction of the

5-nitro group to the corresponding amine, which undergoes P450-catalyzed formation of reactive quinone-imines and forms adducts with hepatic proteins.[53] Accordingly, it was hypothesized that the susceptibility of nitrocatechols to reductive metabolism may be a key determinant of their hepatotoxicity. Thus, using the previously described experimental conditions, DPV and CV experiments were run in negative potentials in order to study the reductive behavior. The results are depicted on Table **4**.

The reductive behavior was studied over the interval +0.25 V and − 1.0 V (Figure **6**). The DPV study showed that at physiological pH compounds **13-16** are reduced ($E_{cp,1}$ ~ −370 mV) to the respective free radical, $RNO_2^{\bullet-}$, in a process involving one electron. The free radical is further reduced ($E_{cp,2}$ ~ −615 mV) to the corresponding hydroxylamine (RNHOH), in a step involving three electrons and four protons (Figure **6**, left). This behavior is consistent with most of the published data found in the literature for the reduction of nitro compounds.[57-59] For the standard COMT inhibitors tolcapone **1** and entacapone **2** only the second cathodic peak ($E_{cp,2}$ ~ −670 mV) was seen (Figure **6A**). CV experiments were also performed for compounds **13-16** and standard COMT inhibitors tolcapone **1** and entacapone **2** (Figure **6B**). Compounds **13-16** exhibit two cathodic signals corresponding to the formation of the nitro radical anion followed by its reduction to the hydroxylamine derivative. An oxidation peak is seen at the reversed scan ($E_{ap,1}$ ~ 95 mV), corresponding to oxidation of the hydroxylamine to the respective nitroso derivative (RNO). For tolcapone **1** and entacapone **2** only one irreversible cathodic peak is seen, which is consistent with the DPV data. Moreover, no peaks were observed in the anodic scan of the voltammogram. However, immediately after the cathodic wave, several subtle reversible reduction peaks can be observed for both compounds. Interestingly, in this case the hydroxylamine derivatives are not as stable as those formed for compounds **13-16**, since oxidation was not observed in the reverse scan. We hypothesize that the unstable hydroxylamines of tolcapone **1** and entacapone **2** may generate other electroactive derivatives, like azoxy or azo derivatives. The formation of these derivatives could have toxicological significance, since these compounds have been associated with mutagenic and and carcinogenic effects in aquatic organisms and humans.[60-63] Contrarily, since the hydroxylamine derivative of

compounds **13-16** is more stable and can be oxidized to the nitroso derivative, the likelihood of formation of azoxy, azo and quinone-imine derivatives is significantly reduced when compared to tolcapone **1** and entacapone **2**. In this sense, this difference in the reductive behavior may explain the increased toxicity observed for tolcapone **1** and entacapone **2**. Further studies are currently being conducted to clarify this hypothesis.

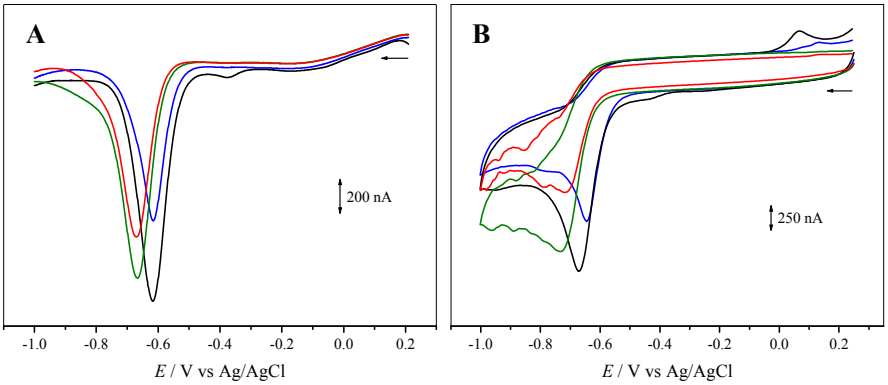

Figure 6. **(A)** Differential pulse voltammograms for 0.1 mM solutions of (—) tolcapone, (—) entacapone, (—) 14 and (—) 16, in physiological pH 7.4 supporting electrolyte. Scan rate: 5 mV s^{-1}; **(B)** Cyclic voltammograms for 0.1 mM solutions of (—) tolcapone, (—) entacapone, (—) 14, (—) 16 and (▪▪▪) CAPE, in physiological pH 7.4 supporting electrolyte. Scan rate: 20 mV s^{-1}.

Docking of compound 16 with rat COMT. The binding interactions of compound **16** (phenethyl-(*E*)-2-cyano-3-(3,4-dihydroxy-5-nitrophenyl)acrylate) was carried out by molecular docking to investigate its binding mode using the crystal structure of rat COMT (pdb id: 2CL5) (Figure **5**). The active site of COMT consists of a ligand binding catalytic site, Mg^{2+} and a co-enzyme binding area with bound SAM.[64] Our studies show that the nitrocatechol ring of compound **16**, was oriented in the catalytic site such that the two hydroxyls were in contact with the magnesium ion (distance = 2.47–2.80 Å). The negatively charged C4 hydroxyl group (mono-ionized form) underwent electrostatic interactions with positively charged NH_3^+ side chain of Lys144 (distance = 1.66 Å) whereas the C3 hydroxyl group underwent hydrogen bonding interactions with Glu199 side chain (distance = 1.89 Å). The nitro-substituent was in

contact via electrostatic interactions with Lys144 side chain (distance = 4.77 Å). The catechol aromatic ring itself was in proximity to Met40 and Pro174 and underwent nonpolar contacts (distance < 5.1 Å). The entire phenethylcyanoacetate substituent was extended away from the catalytic site and oriented toward the solvent area.[65, 66] These observations are consistent with previous reports that show that the presence of a 1,2-dihydroxy-3-nitrobenzene pharmacophore is the primary requirement to exhibit COMT inhibition.

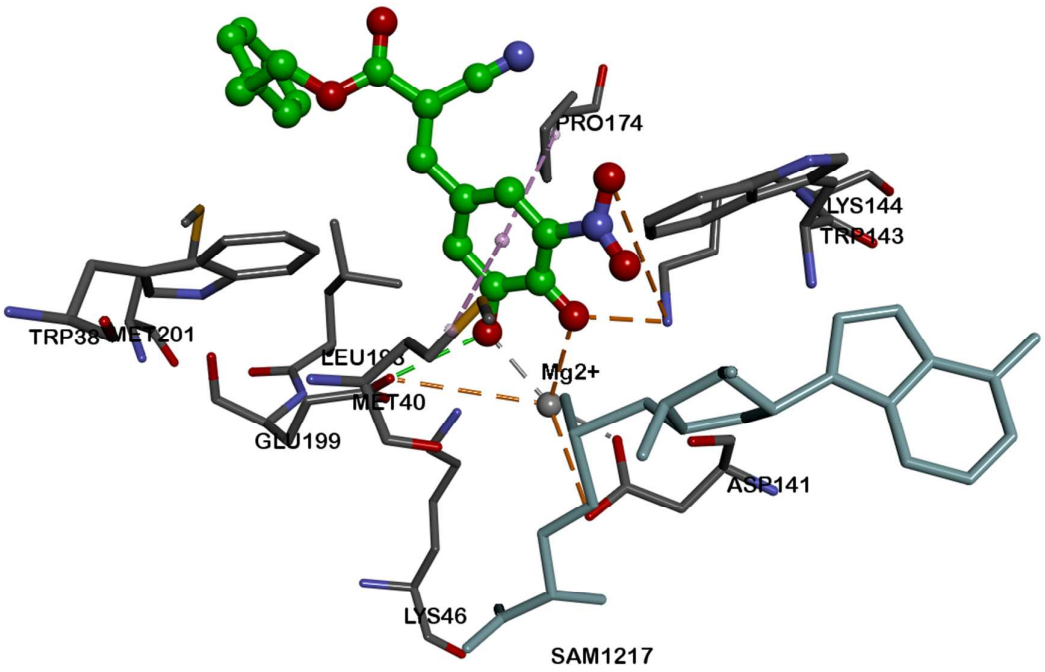

Figure 5. The binding mode of compound **16** in ball and stick cartoon within the rat COMT active site (CDOCKER interaction energy = –61.11 kcal mol-1 and CDOCKER energy = –52.04 kcal mol-1). The hydrogen atoms are not shown to enhance clarity

CONCLUSIONS

New COMT inhibitors based on hydroxycinnamic acid scaffold were successfully developed. Generally, all derivatives bearing a 5-nitro group displayed potent nanomolar inhibion of both COMT isoforms, especially MB-COMT. Moreover, the inhibitory profile was comparable to that observed for standard inhibitors tolcapone and entacapone. Aside from the potent COMT

inhibition, derivatives **13**, **15** and **16** exhibited the appropriate drug-like properties required for CNS drugs and were predicted to be permeable to the BBB, as evaluated by *in vitro* PAMPA-BBB assays. More importantly, derivatives **13**, **15** and **16** did not cause significant toxicity in primary rat hepatocytes in two different viability endpoints (%MTT reduction and %NR uptake > 85%), in contrast with entacapone (% MTT reduction = 51.17 ± 18.87, $p < 0.001$ and % NR uptake= 79.89 ± 16.31, $p < 0.01$) and, especially, tolcapone (% MTT reduction = 9.096 ± 3.263, $p < 0.001$ and % NR uptake = 46.86 ± 8.639, $p < 0.001$). The reduced acidity and different reductive behavior of compounds **13-16**, mainly concerning the reductive stability of the hydroxylamine metabolite, may provide clues as to why these nitrocatechols did not induce hepatoxicity at high micromolar concentrations. In addition, computational docking studies provided insights into the inhibitors' interaction with the enzyme binding site and a rationale for their high potency. The binding mode of **16** suggests that the main interactions with the enzyme's active site are established through the nitrocatechol ring and that the phenethylcyanoacetate moiety extends away from the catalytic site, which enables derivatization of the side chain in order to decrease the risk of hepatotoxicity, improve pharmacokinetics and BBB permeability. Overall, the physico-chemical, pharmacological and toxicological properties of the reported compounds showed that they behave differently from the naturally-occurring scaffolds and cannot be considered pan-assay-interference compounds (PAINS). Overall the results show that the modulation of the chemical structure may enable the development of safe BBB-permeable nitrocatechols without compromising COMT inhibition. Accordingly, compound **16** can be approached as a promising lead for the development of CNS diseases like PD, schizophrenia and other dopamine-deficient associated disorders. Further optimization and characterization within these series will be reported in due course.

EXPERIMENTAL

Chemistry

Reagents, materials and apparatus

All reagents were purchased from Sigma-Aldrich Química S.A. (Sintra, Portugal). Deionised water (conductivity < 0.1 μScm-1) was used for all experiments. All solvents were pro analysis grade and were acquired from Merck (Lisbon, Portugal). Thin layer chromatography (TLC) was performed on precoated silica gel 60 F254 acquired from Merck (Darmstad, Germany) and spots were detected using a UV lamp at 254 nm. Reaction progress was monitored by TLC (dichloromethane/methanol/formic acid, 9:1:0.01). Following the extraction step, subsequent work up of the organic layers included drying over anhydrous sodium sulphate, filtration and elimination of solvents under reduced pressure. Column chromatography was carried out with silica gel 60A acquired from Carlo-Erba Reactifs (SDS, France) or cellulose. The crude products were purified by flash column chromatography and/or recrystallization. The fractions containing the desired product were gathered, concentrated and the product was recrystallized. The elution systems used for flash chromatography and the recrystallization solvents are specified for each compound. Solvents were evaporated with a Buchi Rotavapor. The purity of the final products (>97% purity) was verified by high-performance liquid chromatography (HPLC) equipped with a UV detector. Chromatograms were obtained in an HPLC/DAD system, a Jasco instrument (pumps model 880-PU and solvent mixing model 880-30, Tokyo, Japan), equipped with a commercially prepacked Nucleosil RP-18 analytical column (250 mm x 4.6 mm, 5 μm, Macherey-Nagel, Duren, Germany), and UV detection (Jasco model 875-UV) at the maximum wavelength of 254 nm. The mobile phase consisted of a methanol/water or acetonitrile/water (gradient mode, room temperature) at a flow rate of 1 mL/min. The chromatographic data was processed in a Compaq computer, fitted with CSW 1.7 software (DataApex, Czech Republic).^{1}H, ^{13}C NMR and DEPT135 data were acquired at room temperature on a Brüker AMX 300 spectrometer operating at 400 and 100 MHz, respectively. Chemical shifts were expressed in δ (ppm) values relative to tetramethylsilane (TMS) as internal reference and coupling constants (*J*) were given in Hz. Carbon signals present in DEPT135 spectra were underlined. Mass spectra were obtained on a VG AutoSpec instrument. The data were reported as m/z (% of relative intensity of the most important fragments). Buffer solutions employed for electrochemical studies were 0.1 mol L-1 in the pH range 1.2-12.2.

General procedure for Knoevenagel-Doebner condensation (Scheme 1, step a)

A mixture of 3,4-dihydroxy-5-nitrobenzaldehyde (1 mmol) and the appropriate activated methylene (malonic acid, cyanoacetic acid, ethylmalonate or diethylmalonate, 2 mmol) in anhydrous pyridine (9.6 mmol) and catalytic amount of piperidine was stirred at 60˚C. The reaction mixture was then cooled at 0˚C, poured over ice water, neutralized with HCl 1M and extracted with ethyl acetate (3 x 10 mL). The combined organic layers were then washed with water (10 mL) and brine (2 x 10 mL). The product was purified by column chromatography and/or recrystallization. The procedure was adapted from Gaspar *et al.* 2009.[55]

(E)-3-(3,4-Dihydroxy-5-nitrophenyl)acrylic acid (8)

Compound **8** was obtained in the following conditions: 3,4-dihydroxy-5-nitrobenzaldehyde (0.25 g, 1.81 mmol), malonic acid (0.38 g, 3.62 mmol), anhydrous pyridine (1.45 mL, 18.10 mmol), piperidine (4 drops) for 48h. Compound **8** was purified by column chromatography (dichloromethane/methanol (9:1) until (8:2)) and recrystallization from ethyl ether/petroleum ether as a yellow solid. η = 40 %. ^{1}H NMR (400 MHz, MeOD) δ 7.76 (d, *J* = 2.0 Hz, 1H, H6), 7.58 (d, *J* = 15.9 Hz, 1H, Hβ), 7.39 (d, *J* = 2.1 Hz, 1H, H2), 6.40 (d, *J* = 15.9 Hz, 1H, Hα). ^{13}C NMR (100 MHz, MeOD) δ 169.54, 149.20, 145.94, 143.69, 136.06, 126.72, 118.98, 118.87, 116.65. EI-MS: *m/z* 225 ($M^{\bullet+}$).

(E)-2-Cyano-3-(3,4-dihydroxy-5-nitrophenyl)acrylic acid (9)

Compound **9** was obtained by following a Knoevenagel-Doebner condensation between 3,4-dihydroxy-5-nitrobenzaldehyde and malonic acid in the following conditions: 3,4-dihydroxy-5-nitrobenzaldehyde (0.50 g, 2.73 mmol), cyanoacetic acid (0.47 g, 5.46 mmol), anhydrous pyridine (2.19 mL, 21.3 mmol), piperidine (5 drops) for 24h. Compound **9** was recrystallized from acetone /petroleum ether as a yellow solid. η = 64.05 %. ^{1}H NMR (400 MHz, MeOD) δ 8.18 (s, 1H, Hβ), 8.17 (m, 1H, H(Ar)), 7.89 (d, *J* = 2.2 Hz, 1H, H(Ar)). ^{13}C NMR (101 MHz, MeOD) δ 164.41, 153.31, 149.34, 147.72, 136.42, 123.63, 120.75, 120.47, 116.18, 103.37. EI-MS: *m/z* 250 ($M^{\bullet+}$).

Ethyl (E)-3-(3,4-dihydroxy-5-nitrophenyl)acrylate (10)

Compound **10** was obtained in the following conditions: 3,4-dihydroxy-5-nitrobenzaldehyde (0.500 g, 2.73 mmol), ethyl malonate (0.644 mL, 5.461 mmol), anhydrous pyridine (2.2 mL, 27.3 mmol), piperidine (4 drops) for 24 hours. Compound **10** was recrystallized from diethyl ether as a yellow solid. η = 67.44 %. ^{1}H NMR (400 MHz, DMSO-d_6) δ 10.56 (s, 2H, 2xOH), 7.71 (d, J = 2,0 Hz, 1H, H6), 7.55 (d, J = 16.0 Hz, 1H, Hβ), 7.36 (d, J = 2.0 Hz, 1H, H2), 6.43 (d, J = 16.0 Hz, 1H, Hα), 4.17 (q, J = 7.1 Hz, 2H, C$\underline{H}_2$CH$_3$), 1.25 (t, J = 7.1 Hz, 3H, CH$_2$C$\underline{H}_3$). ^{13}C NMR (101 MHz, DMSO-d_6) δ 166.52, 148.37, 143.97, 143.26, 138.03, 125.28, 118.02, 117.89, 116.37, 60.47, 14.64. EI-MS: m/z 270 ($M^{\bullet+}$).

Diethyl 2-(3,4-dihydroxy-5-nitrobenzylidene)malonate (11)

Compound **11** was obtained in the following conditions: 3,4-dihydroxy-5-nitrobenzaldehyde (1g, 5.461 mmol), diethyl malonate (1.658 mL, 10.922 mmol), anhydrous pyridine (4.202 mL, 52.426 mmol), piperidine (5 drops) for 7 hours. The crude product was purified by flash chromatography with dichloromethane/methanol (9.5:0.5). η = 69.01 %. ^{1}H NMR (400 MHz, DMSO-d_6) δ 10.82 (bs, 2H, 2xO$\underline{H}$), 7.61 (m, 2H, H6, Hβ), 7.35 (d, J = 1.9 Hz, 1H, H(2)), 4.32 (q, J = 7.1 Hz, 2H, OC$\underline{H}_2$CH$_3$)), 4.23 (q, J = 7.1 Hz, 2H, OC$\underline{H}_2$CH$_3$)), 1.23 (m, 6H, 2x(OCH$_2$C$\underline{H}_3$)).^{13}C NMR (101 MHz, DMSO-d_6) δ 166.38, 163.90, 148.49, 144.87, 140.25, 137.66, 122.88, 125.07, 118.63, 118.28, 62.05, 61.82, 14.44, 14.12. EI-MS m/z 326 ($M^{\bullet+}$).

2-(3,4-Dihydroxy-5-nitrobenzylidene)malonic acid (12) (Scheme 1, step b)

Compound **12** was obtained by hydrolysis of compound **11** with aqueous NaOH 2M. Briefly, a solution of compound **11** (0.20 g, 0,62 mmol) in MeOH (2 mL) and THF (12 mL) was treated with aqueous NaOH 2M (1 mL) and refluxed for 13 hours. The solvents were removed by reduced pressure and the crude residue was suspended in water (10 mL) and acidified with concentrated HCl. The solution was then extracted with ethyl acetate (3 x 20 mL) and the organic layer was washed with brine (3 x 10 mL), dried over Na_2SO_4, filtered and concentrated under reduced pressure. The crude product was recrystallized from dichloromethane. η = 27.9

%. ^{1}H NMR (400 MHz, DMSO-d_6) δ 13.26 (bs, 2H, 2xCOOH)), 10.62 (bs, 2H, 2xOH), 7.64 (d, J = 2.2 Hz, 1H, H6), 7.42 (s, 1H, Hβ), 7.350 (d, J = 2.1 Hz, 1H, H2). ^{13}C NMR (101 MHz, DMSO-d_6) δ 168.19, 165.60, 148.32, 144.03, 137.77, 137.49, 127.98, 123.77, 119.50, 117.32. EI-MS *m/z* 270 ($M^{\bullet+}$).

General procedure for the preparation of benzyl and phenethyl esters (Scheme 1, step c)

The hydroxycinnamic acid with the appropriate substitution pattern (1 mmol) was dissolved in DMSO (3 mL), K_3PO_4 (1.2 mmol) was added slowly and the mixture was stirred for 30 minutes at room temperature. A solution of the appropriate alkyl bromide (benzyl bromide or (2-bromoethyl)benzene, 1.02 mmol) in DMSO was then added dropwise and the mixture was stirred for 24 hours at room temperature. Upon completion the mixture was poured dropwise into ice water (20 mL), left to stir for 1 hour and extracted with ethyl acetate (3 x 10 mL). The combined organic layers were then acidified with HCl 1M and washed with water (3 x 10 mL) and brine (3 x 10 mL), dried over anhydrous sodium sulphate and concentrated. The compound was purified by recrystallization. The procedure was adapted from Liu *et al.* 2012.[67]

Phenethyl (E)-3-(3,4-dihydroxyphenyl)acrylate (CAPE, 6)

Compound **6** was obtained in the following conditions: caffeic acid (0.30 g, 1.66 mmol) in DMSO (3.15 mL), K_3PO_4 (0.43 g, 2.00 mmol), (2-bromoethyl)benzene (0.24 mL, 1.70 mmol) in DMSO (1.05 mL). Compound **6** was recrystallized from ethyl acetate/petroleum ether as a light yellow solid. η = 48 %. ^{1}H NMR (400 MHz, DMSO-d_6) δ 9.27 (s, 2H, 2xOH), 7.45 (d, J = 15.9 Hz, 1H, Hβ), 7.31 (m, 4H, H2', H3', H5', H6'), 7.22 (m, 1H, H4'), 7.03 (d, J = 2.03 Hz, 1H, H2), 6.99 (dd, J = 8.2, 2.0 Hz, 1H, H6), 6.76 (d, J = 8.1 Hz, 1H, H5), 6.23 (d, J = 15.9 Hz, 1H, Hα), 4.32 (t, J =6.0 Hz, 2H, $COOCH_2$), 2.95 (t, J = 6.9 Hz, 2H, CH_2Ph). ^{13}C NMR (100 MHz, DMSO-d_6) δ 166.9, 148.9, 146.0, 145.7, 138.5, 129.4, 128.8, 126.8, 125.9, 121.7, 116.2, 115.3, 114.3, 64.8, 35.0. EI-MS *m/z* 284 ($M^{\bullet+}$).

Benzyl (E)-3-(3,4-dihydroxyphenyl)acrylate (7)

Compound **7** was obtained in the following conditions: caffeic acid (0.50 g, 1.67 mmol) in DMSO (4 mL), K_3PO_4 (0.43 g, 2.00 mmol), benzyl bromide (0.20 mL, 1.70 mmol) in DMSO (1 mL). Compound **7** was recrystallized from ethyl acetate/petroleum ether as a light yellow solid. η = 80.54 %. ^{1}H NMR (400 MHz, DMSO-d_6) δ 7.57 (d, J = 15.9 Hz, 1H, Hβ), 7.42 – 7.27 (m, 4H, H2'-H5'), 7.04 (d, J = 2.1 Hz, 1H, H2), 6.94 (dd, J = 8.2, 2.0 Hz, 1H, H5), 6.77 (d, J = 8.2 Hz, 1H, H6), 6.30 (d, J = 15.9 Hz, 1H, Hα), 5.21 (s, 2H, C$\underline{H_2}$). ^{13}C NMR (100 MHz, DMSO-d_6) δ 167.61, 148.25, 145.81, 145.42, 136.46, 128.15, 127.77, 127.75, 126.31, 121.61, 115.10, 113.77, 113.55, 65.75. EI-MS *m/z* 269.7 ($M^{\bullet+}$).

Benzyl (E)-3-(3,4-dihydroxy-5-nitrophenyl)acrylate (13)

Compound **13** was obtained in the following conditions: compound **8** (0.20 g, 0.89 mmol) in DMSO (2.2 mL), K_3PO_4 (0.28 g, 1.07 mmol) and benzyl bromide (0.11 mL, 0.91 mmol) in DMSO (0.56 mL). η = 29.47 %. ^{1}H NMR (400 MHz, DMSO-d_6) δ 10.52 (s, 2H, 2xOH), 7.73 (d, J = 1.9 Hz, 1H, H6), 7.61 (d, J = 16.0 Hz, 1H, Hβ), 7.38 (m, 6H, H2'-6', H2), 6.50 (d, J = 16.0 Hz, 1H, Hα), 5.22 (s, 2H, CH_2). ^{13}C NMR (100 MHz, DMSO-d_6) δ 166.47, 152.30, 148.38, 146.89, 143.79, 136.72, 128.92, 128.81, 128.47, 125.18, 120.12, 116.55, 114.45, 66.00. EI-MS *m/z* 315 ($M^{\bullet+}$).

Phenethyl (E)-3-(3,4-dihydroxy-5-nitrophenyl)acrylate (14)

Compound **14** was obtained in the following conditions: compound **8** (0.20 g, 0.89 mmol) in DMSO (2.2 mL), K_3PO_4 (0.28 g, 1.07 mmol) and (2-bromoethyl)benzene (0.13 mL, 0.91 mmol) in DMSO (0.56 mL). Compound **14** was recrystallized from ethyl acetate/petroleum ether as a yellow solid. η = 30.7 %. ^{1}H NMR (400 MHz, DMSO-d_6) δ 10.51 (s, 2H, 2xOH), 7.71 (d , J = 2.0 Hz, 1H, H6), 7.54 (d, J = 16.0 Hz, 1H, Hβ), 7.35 (d, J = 2.1 Hz, 1H, H2), 7.30 (m, 4H, H2', H3', H5', H6'), 7.23 (m, 1H, H4'), 6.42 (d, J = 16.0 Hz, 1H, Hα), 4.35 (t, J = 6.8 Hz, 2H, $COOCH_2$), 2.96 (t, J = 6.8 Hz, 2H, CH_2Ph). ^{13}C NMR (100 MHz, DMSO-d_6) δ 166.5, 148.5, 144.3, 138.5, 138.0, 129.4, 128.9, 126.9, 125.0, 117.9, 117.6, 116.5, 65.1, 34.9. EI-MS *m/z* 329 ($M^{\bullet+}$).

Benzyl (E)-2-cyano-3-(3,4-dihydroxy-5-nitrophenyl)acrylate (15)

Compound **15** was obtained in the following conditions: compound **9** (0.30 g, 1.20 mmol) in DMSO (3 mL), K_3PO_4 (0.31 g, 1.44 mmol) and benzyl bromide (0.15 mL, 1.22 mmol) in DMSO (0.70 mL). Compound **15** was recrystallized from ethyl acetate/petroleum ether. η = 45.04 %. ^{1}H NMR (400 MHz, MeOD) δ 8.23 (s, 1H, Hβ), 8.18 (d, *J* = 2.0 Hz, 1H, H6), 7.89 (d, J = 2.2 Hz, 1H, H2), 7.40 (m, 5H, H2'-H6'), 5.35 (s, 2H, CH_2). ^{13}C NMR(100 MHz, DMSO-d_6) δ 162.55, 154.19, 148.19, 148.74, 137.62, 135.93, 129.01, 128.97, 128.49, 116.36, 67.42. EI-MS *m/z* 340 ($M^{\bullet+}$).

Phenethyl (E)-2-cyano-3-(3,4-dihydroxy-5-nitrophenyl)acrylate (16)

Compound **16** was obtained in the following conditions: compound **9** (0.18 g, 0.47 mmol) in DMSO (0.90 mL), K_3PO_4 (0.12 g, 0.56 mmol) and (2-bromoethyl)benzene (0.065 mL, 0.48 mmol) in DMSO (0.30 mL). Compound **16** was recrystallized from ethyl acetate/petroleum ether as a yellow solid. η = 29.0 %. ^{1}H NMR (400 MHz, DMSO-d_6) δ 8.24 (s, 1H, Hβ), 8.09 (d, *J* = 2.1 Hz, 1H, H6), 7.87 (d, *J* = 2.1 Hz, 1H, H2), 7.32 (m, 4H, H2', H3', H5', H6'), 7.24 (m, 1H, H4'), 4.45 (t, *J* = 6.8 Hz, 2H, $COOCH_2$), 3.01 (t, *J* = 6.8 Hz, 2H, CH_2Ph). ^{13}C NMR (100 MHz, DMSO-d_6) δ 164.5, 153.9, 148.8, 147.6, 138.1, 137.8, 129.5, 128.6, 127.0, 121.8, 121.6, 118.1, 116.1, 100.22, 67.0, 34.7. EI-MS *m/z* 354 ($M^{\bullet+}$).

General procedure for PyBOP-assisted amidation (Scheme 1, step d)

The hydroxycinnamic acid with the appropriate aromatic substitution (1 mmol) was dissolved in diisopropylethylamine (1 mmol) and dimethylformamide (2 mL). The reaction was placed on ice, PyBOP (1 mmol) in dichloromethane (2 mL) was added and the mixture was stirred for 30 minutes. The amine (1 mmol) was then added, the mixture was allowed to reach room temperature and stirred for an additional 6 hours. The solvents were removed under reduced pressure and the residue was dissolved in ethyl acetate (30 mL). The solution was washed with water (3 x 10 mL), HCl 1M (3 x 10 mL) and brine (10 mL). The final products were purified by recrystallization. The procedure was adapted from Gaspar *et al.* 2011.[68]

(E)-N-Benzyl-2-cyano-3-(3,4-dihydroxy-5-nitrophenyl)acrylamide (17)

Compound **17** was obtained in the following conditions: compound **9** (0.20 g, 0.80 mmol), benzylamine (0.088 mL, 0.81 mmol), PyBOP (0.42 g, 0.81 mmol), diisopropylethylamine (0.14 mL, 0.81 mmol) in dimethylformamide (2 mL) and dichloromethane (2 mL). Compound **17** was recrystallized from dichloromethane/petroleum ether as a yellow solid. η = 25.8 %. ^{1}H NMR (400 MHz, DMSO-d_6) δ 8.91 (t, J = 5.9 Hz, 1H, NH), 8.08 (s, 1H, Hβ), 7.95 (d, J = 2.1 Hz, 1H, H6), 7.77 (d, J = 2.2 Hz, 1H, H2),7.34 (m, 4H, HAr), 7.26 (m, 1H, H4'), 4.42 (d, J = 5.9 Hz, 2H, CH_2). ^{13}C NMR (100 MHz, DMSO-d_6) δ 161.8, 149.6, 149.0, 148.9, 139.4, 137.5, 128.8, 127.9, 127.4, 120.6, 117.5, 117.0, 43.6. EI-MS: *m/z* 340 ($M^{\bullet+}$).

(E)-2-Cyano-3-(3,4-dihydroxy-5-nitrophenyl)-N-phenethylacrylamide (18)

Compound **18** was obtained in the following conditions: compound **9** (0.20 g, 0.80 mmol), phenethylamine (0.11 mL, 0.81 mmol), PyBOP (0.42 g, 0.81 mmol), diisopropylethylamine (0.14 mL, 0.81 mmol) in dimethylformamide (2 mL) and dichloromethane (2 mL). Compound **18** was recrystallized from acetone/*n*-hexane as a yellow solid. η = 15.9 %. ^{1}H NMR (400 MHz, DMSO-d_6) δ10.90 (brs, 2H, 2xOH), 8.02 (t, J = 5.4 Hz, 1H, NH), 8.00 (s, 1H, Hβ), 7.94 (d, J = 1.8 Hz, 1H, H6), 7.77 (d, J = 2.2 Hz, 1H, H2),7.16 (m, 5H, HAr), 3.43 (m, 2H, CH_2), 2.82 (t, J = 7.4 Hz, 2H, CH_2). ^{13}C NMR (100 MHz, DMSO-d_6) δ 161.4, 149.2, 148.7, 139.7, 137.7, 136.6, 129.1, 128.98, 126.6, 122.3, 119.9, 118.3, 116.8, 104.8, 41.8, 35.32. EI-MS: *m/z* 354 ($M^{\bullet+}$).

Pharmacology

Animals. Male Wistar rats obtained from Harlan (Barcelona, Spain) were used. Rats were kept 8 per cage, under controlled environmental conditions (12 hours light/dark cycle and room temperature 22 ± 1ºC) with food and tap water allowed *ad libitum*. Twenty minutes before sacrifice animals were anesthetized with sodium pentobarbital (60 mg/kg) administered intraperitoneally. After sample collection anaesthetized animals were euthanized by

decapitation. All experiments were approved by the local Ethics Committee for the welfare of experimental animals and performed in accordance with national legislation.

Homogenate Preparation. Tissues were thawed at room temperature and homogenized using a Diax homogenizer (Heidolph, 2 cycles of 20 s in position 5, on ice). Total protein content in homogenates was measured with Bio-Rad standard protein assay using a standard curve of bovine serum albumin (50-250 μg/mL). Samples were then diluted to obtain a concentration of 4 mg/mL.

COMT Activity Determination. COMT activity was evaluated by the ability to methylate adrenaline to metanephrin, as previously described.[35] Aliquots of 100 μL of liver or brain homogenates (2mg/mL protein) were preincubated for 20 min with 80 μL of test compounds in phosphate buffer 5mM containing pargyline (100 μM), $MgCl_2$ (100 μM) and ethylene glycol tetracetic acid (EGTA, 1 mM) and saturating concentrations of SAM (500 μM for liver homogenates and 100 μM for brain homogenates). For experiments with liver homogenates, the reaction was started with the addition of adrenaline (1000 μM) and incubated for 5 min. For experiments with brain homogenates, the reaction was started with the addition of adrenaline (5 μM) and incubated for 15 min. The preincubation and incubation were carried out at 37˚C, in conditions of light protection, with continuous shaking and without oxygenation. At the end of the incubation period the reaction was stopped by the addition of 50 μL of 2 M perchloric acid and the tubes were transferred to ice. The samples were then centrifuged (200g, 4 min, 4˚C), and 250 μL aliquots of the supernatant filtered on 0.22 μm pore size Spin-X filter tubes Costar. Aliquots of 50 μL of the filtered supernatant were injected into the chromatograph. The chromatography system consisted of a pump Gilson model 302 (Gilson Medical Electronics,Villiers le Bel, France) connected to a manometric module (Gilson model 802 C). and a stainless steel 5 mm ODS column (Biophase; Bioanalytical Systems, West Lafayette, IN.) of 25 cm length; samples were injected by means of an automatic sample injector (Gilson model 234). The mobile phase was a degassed solution of citric acid (0.1 mM), sodium octylsulphate (0.5 mM), sodium acetate (0.1 M), EDTA (0.17mM), dibutylamine (1 mM). and methanol 6%

(*v*/*v*), adjusted to pH 3.5 with perchloric acid 2 M. and pumped at a rate of 1.0 ml/min. The detection was carried out electrochemically with a glassy carbon electrode, an Ag/AgCl reference electrode and an amperometric detector Gilson (model 141); the detector cell was operated at 0.75 V. The current produced was monitored using the Gilson 712 HPLC software. The lower limits for detection of metanephrine ranged from 350 to 500 fmol. For the calculation of the IC_{50} the parameters of the equation for one site inhibition were fitted to the experimental data.

CNS penetration: in vitro parallel artificial membrane permeability assay (PAMPA-BBB)

Prediction of the brain penetration was evaluated using a parallel artificial membrane permeability assay (PAMPA). Ten commercial drugs, phosphate buffer saline solution at pH 7.4 (PBS), ethanol and dodecane were purchased from Sigma, Acros organics, Merck, Aldrich and Fluka. The porcine polar brain lipid (PBL) (catalog no. 141101) was from Avanti Polar Lipids. The donor plate was a 96-well filtrate plate (Multiscreen® IP Sterile Plate PDVF membrane, pore size is 0.45 μM, catalog no. MAIPS4510) and the acceptor plate was an indented 96-well plate (Multiscreen®, catalog no. MAMCS9610), both from Millipore. Filter PDVF membrane units (diameter 30 mm, pore size 0.45 μm) from Symta were used to filter the samples. A 96-well plate UV reader (Thermoscientific, Multiskan spectrum) was used for the UV measurements. Commercially available compounds with known permeability (caffeine, enoxacine, hydrocortisone, desipramine, ofloxacine, piroxicam, testosterone, promazine, verapamil and atenolol) and test compounds were dissolved in PBS:ethanol (7:3) and filtered. The acceptor 96-well microplate was filled with 180 μL of PBS/EtOH (70/30). The donor 96-well plate was coated with 4 μL of porcine brain lipid in dodecane (20 $mg \cdot mL^{-1}$) and after 5 minutes, 180 μL of each compound solution was added. The donor plate was carefully put on the acceptor plate to form a "sandwich", which was left undisturbed for 2h and 30 min at 25 °C. During this time the compounds diffused from the donor plate through the brain lipid membrane into the acceptor plate. After incubation, the donor plate was removed. The concentrations of the commercial drugs and the test compounds in the acceptor and donor wells were determined

spectrophotometrically in a UV plate reader. Every sample was analyzed at three to five wavelengths, in 3 wells and in two independent runs. Results are given as the mean ± standard deviation (SD) and the average of the two runs is reported. Ten quality control compounds with known BBB permeability were included in each experiment to validate the analysis set.

***In vitro* toxicology**

All reagents used were of analytical grade or of the highest grade available. Neutral red (NR) solution, (4,5-dimethylthiazol-2-yl)-2,5-diphenyl tetrazolium (MTT) bromide, trypan blue solution [0.4 % (w/v)] and William's E medium were obtained from Sigma (St. Louis, MO, USA). Reagents used in cell culture, including heat inactivated fetal bovine serum (FBS), antibiotic (10000 U/mL penicillin, 10000 µg/mL streptomycin), phosphate-buffered saline solution (PBS) and Hank's balanced salt solution (HBSS) were purchased from Gibco Laboratories (Lenexa, KS). Dimethylsulfoxide (DMSO), absolute ethanol and acetic acid were obtained from Merck (Darmstadt, Germany).

Isolation and primary culture of rat hepatocytes. Rat hepatocytes were isolated from male Wistar Han rats (200 – 250 g) purchased from Charles-River Laboratories (Barcelona, Spain). All experiments were approved by the local Ethics Committee for the welfare of experimental animals and performed in accordance with national legislation. Surgical procedures were conducted under anesthesia by inhalation of isoflurane, in an isolated system, and carried out between 10.00 and 11.00 a.m. Cells were isolated through a collagenase perfusion, as previously described by our group.[69] Briefly, a cannula was inserted in the hepatic portal vein, and the liver was perfused initially with Hank's washing buffer containing bovine serum albumin (BSA) and the chelating agent EGTA, followed by a solution of collagenase supplemented by its co-factor calcium. The liver capsule was then gently disrupted in order to release isolated liver cells into a Krebs-Henseleit buffer. The cell suspension was subsequently purified through three cycles of low-speed centrifugations (300 rpm, for 2 min). The final suspension was then incubated with penicillin/streptomycin (500 U/mL / 500 µg/mL), at 4ºC,

for 30 min. Cell viability was estimated by the trypan blue exclusion test and was always higher than 80%. A suspension of 500.000 viable cells/mL was cultured in 96-well plates at approximately 100.000 cells/cm^2, in William's E medium, supplemented with 10% FBS (100 U/mL), penicillin/streptomycin (100 μg/mL), insulin (5 μg/mL), dexamethasone (50 μM), gentamicin (100 μg/mL) and fungizone (2.5 μg/mL), and incubated overnight at 37˚C, with 5% CO_2, to allow cell adhesion.

MTT reduction assay. The MTT reduction assay was used to measure mitochondrial dysfunction (decrease in mitochondrial dehydrogenase activity) in rat primary hepatocytes exposed to the test compounds. The signal generated is dependent on the degree of reduction of the MTT tetrazolium salt (water soluble) to MTT formazan (water insoluble) by cellular dehydrogenases within metabolically active cells. Briefly, 24h after seeding at 100.000 cells/cm^2 the cells were exposed to the test compounds (0, 1, 10 and 50 μM) in cell culture medium without FBS for 24 h. At the selected time point, the cell culture medium was removed, followed by the addition of fresh cell culture medium containing 0.5 mg/mL MTT and incubation at 37 °C in a humidified, 5% CO_2-95% air atmosphere for 1 h. After this incubation period, the cell culture medium was removed and the formed formazan crystals dissolved in 100% DMSO. The absorbance was measured at 550 nm in a multi-well plate reader (BioTek Instruments, Vermont, USA). The percentage of MTT reduction relative to that of the control cells was used as the cytotoxicity measure [MTT reduction (% of control)].

Neutral red uptake assay. The NR uptake assay is based on the ability of viable cells to incorporate and bind the supravital dye neutral red in the lysosomes, thus providing a quantitative estimation of the number of viable cells in a culture. Briefly, 24h after seeding at 100.000 cells/cm^2 the cells were exposed to the test compounds (0, 1, 10 and 50 μM) in cell culture medium without FBS for 24 h. At the selected time point, the cell culture medium was removed and the cells incubated with neutral red (50 μg/mL in cell culture medium) at 37 °C, in a humidified, 5% CO_2-95% air atmosphere, for 1 h. After this incubation period, the cell culture medium was removed, the dye absorbed only by viable cells extracted [with absolute ethyl

alcohol /distilled water (1:1) containing 5% acetic acid], and the absorbance measured at 540 nm in a multi-well plate reader (BioTek Instruments, Vermont, USA). The percentage of NR uptake relative to that of the control cells was used as the cytotoxicity measure [NR uptake (% of control)].

Electrochemical studies

Voltammetric measurements were performed using an Autolab PGSTAT 12 potentiostat/galvanostat (Metrohm-Autolab, Netherlands) in a one-compartment glass electrochemical cell equipped with a three–electrode system arrangement composed of a platinum wire as auxiliary electrode, a Ag/AgCl (saturated KCl) electrode as reference, and a glassy carbon electrode (GCE, d = 2 mm) as working electrode. All measurements were carried out at room temperature (25 ± 1 ºC) and purified nitrogen was used for oxygen displacement. The working electrode was polished manually with an aqueous slurry of alumina powder (BDH Chemicals, VWR, USA) on a microcloth pad and rinsed with water before use. The pH measurements were performed using a Crison pH-meter (Crison, Spain) equipped with a glass pH electrode.

Statistical analysis

Statistical comparisons between control and test groups were carried by one-way analysis of variance (ANOVA-1) followed by Bonferroni's multiple comparison post-test ($\alpha = 0.05$, 95% confidence intervals) using GraphPad Prism 5 ®.

Molecular docking studies

The molecular docking studies were carried out using the computational software Discovery Studio (DS): Structure-Based-Design, version 4.5.1.15071, 2005-2015 (BIOVIA, San Diego, USA). The coordinates for the rat COMT monomer were obtained from pdb (id: 2CL5). All the water molecules except the H2205, which is coordinated to Mg^{2+}, were removed. The enzyme

was prepared using the macromolecules module in DS which provided all the amino acids in their physiological ionization states. The catalytic Lys144 was in its protonated state (ε-amino group). Compound **16** was built in its mono-ionized form (negative charge on C4 hydroxyl group of the catechol ring) using the small molecules module in DS. The binding site was defined by selecting a 15 Å sphere radius around the ligand BIE1218 bound to COMT.[66] Then the ligand BIE1218 was deleted. The docking was performed using the CDOCKER algorithm in the receptor-ligand interactions module which is based on simulated annealing protocol (2000 heating steps, 700 K heating target temperature and 5000 cooling steps, 300 K cooling target temperature) that generated ten docked poses. The CHARMm force field was used for docking studies. The poses obtained were ranked based on CDOCKER interaction energy and CDOCKER energy parameters in kcal·mol^{-1}. The polar and nonpolar contacts of the ligand with the COMT catalytic site were evaluated.

ANCILLIARI INFORMATION

Supporting information. Supporting Information Available: NMR spectra, *in vitro* COMT inhibition, PAMPA-BBB assay validation.

Corresponding Author Information. Fernanda Borges. Phone: +351 220402560. E-mail: fborges@fc.up.pt.

Abbreviations. CAPE: caffeic acid phenethyl ester. COMT: catechol *O*-methyltransferase. CNS: central nervous system. DPV: differential pulse voltammetry. HCA: hydroxycinnamic acid. GSH: glutathione. L-DOPA: levodopa. E_{ap}: anodic electrochemical potential. E_{cp}: cathodic electrochemical potential. LE: ligand efficiency. LELP: ligand-efficiency-dependent lipophilicity. LLE: ligand-lipophilicity efficiency. (MB)-COMT: membrane bound COMT. MTT: methylthiazolyldiphenyl-tetrazolium bromide. NR: neutral red. P450: cytochrome P450. PD:Parkinson's disease. *Pe*: in vitro permeabilities. (S)-COMT: soluble COMT. SAH: *S*-adenosyl-*L*-homocysteine. SAM: *S*-adenosylmethionine. tPSA: topological polar surface area.

Acknowledgements. This project was supported by Foundation for Science and Technology (FCT), and FEDER/COMPETE (UID/QUI/00081/2015, POCI-01-0145-FEDER-006980, and NORTE-01-0145-FEDER-000028). The authors also thank the COST action CA15135 (Multi-target paradigm for innovative ligand identification in the drug discovery process MuTaLig) for support. T. Silva (SFRH/BD/79671/2011) grant was also supported by FCT and FEDER/COMPETE funds. Ontario Mental Health Foundation (graduate scholarship for TM), NSERC-Discovery (RGPIN: 03830-2014); Canada Foundation for Innovation (CFI-JELF); Ontario Research Fund (ORF) and Early Researcher Award (ERA), Ministry of Research and Innovation, Government of Ontario, Canada (PPNR) are also acknowledged for financial support of this research project.

REFERENCES

1. Guldberg, H. C.; Marsden, C. A. Catechol-O-methyl transferase: pharmacological aspects and physiological role. *Pharmacol. Rev.* **1975,** *27*, 135-206.

2. Myohanen, T. T.; Schendzielorz, N.; Mannisto, P. T. Distribution of catechol-O-methyltransferase (COMT) proteins and enzymatic activities in wild-type and soluble COMT deficient mice. *J. Neurochem.* **2010,** *113*, 1632-1643.

3. Tilgmann, C.; Melen, K.; Lundstrom, K.; Jalanko, A.; Julkunen, I.; Kalkkinen, N.; Ulmanen, I. Expression of recombinant soluble and membrane-bound catechol O-methyltransferase in eukaryotic cells and identification of the respective enzymes in rat brain. *Eur. J. Biochem.* **1992,** *207*, 813-821.

4. Ellingson, T.; Duddempudi, S.; Greenberg, B. D.; Hooper, D.; Eisenhofer, G. Determination of differential activities of soluble and membrane-bound catechol-*O*-methyltransferase in tissues and erythrocytes. *J. Chromatogr. B Biomed. Sci. Appl.* **1999,** *729*, 347-353.

5. Axelrod, J.; Senoh, S.; Witkop, B. *O*-Methylation of catechol amines in vivo. *J. Biol. Chem.* **1958,** *233*, 697-701.

6. Axelrod, J.; Tomchick, R. Enzymatic O-methylation of epinephrine and other catechols. *J. Biol. Chem.* **1958,** *233*, 702-705.

7. Yager, J. D.; Liehr, J. G. Molecular mechanisms of estrogen carcinogenesis. *Annu. Rev. Pharmacol. Toxicol.* **1996,** *36*, 203-232.

8. Zhu, B. T.; Ezell, E. L.; Liehr, J. G. Catechol-*O*-methyltransferase-catalyzed rapid *O*-methylation of mutagenic flavonoids. Metabolic inactivation as a possible reason for their lack of carcinogenicity in vivo. *J. Biol. Chem.* **1994,** *269*, 292-299.

9. Calne, D. B. Treatment of Parkinson's disease. *N. Engl. J. Med.* **1993,** *329*, 1021-1027.

10. Endres, C. J.; DeJesus, O. T.; Uno, H.; Doudet, D. J.; Nickles, J. R.; Holden, J. E. Time profile of cerebral [^{18}F]6-fluoro-L-DOPA metabolites in nonhuman primate: implications for the kinetics of therapeutic L-DOPA. *Front. Biosci.* **2004,** *9*, 505-512.

11. Buddhala, C.; Loftin, S. K.; Kuley, B. M.; Cairns, N. J.; Campbell, M. C.; Perlmutter, J. S.; Kotzbauer, P. T. Dopaminergic, serotonergic, and noradrenergic deficits in Parkinson disease. *Ann. Clin. Trans. Neurol.* **2015,** *2*, 949-959.

12. Chaudhury, D.; Walsh, J. J.; Friedman, A. K.; Juarez, B.; Ku, S. M.; Koo, J. W.; Ferguson, D.; Tsai, H. C.; Pomeranz, L.; Christoffel, D. J.; Nectow, A. R.; Ekstrand, M.; Domingos, A.; Mazei-Robison, M. S.; Mouzon, E.; Lobo, M. K.; Neve, R. L.; Friedman, J. M.; Russo, S. J.; Deisseroth, K.; Nestler, E. J.; Han, M. H. Rapid regulation of depression-related behaviours by control of midbrain dopamine neurons. *Nature* **2013,** *493*, 532-536.

13. Goldman-Rakic, P. S.; Castner, S. A.; Svensson, T. H.; Siever, L. J.; Williams, G. V. Targeting the dopamine D1 receptor in schizophrenia: insights for cognitive dysfunction. *Psychopharmacology* **2004,** *174*, 3-16.

14. Aarts, E.; van Holstein, M.; Hoogman, M.; Onnink, M.; Kan, C.; Franke, B.; Buitelaar, J.; Cools, R. Reward modulation of cognitive function in adult attention-deficit/hyperactivity disorder: a pilot study on the role of striatal dopamine. *Behav. Pharmacol.* **2015,** *26*, 227-240.

15. Kiss, L. E.; Soares-da-Silva, P. Medicinal chemistry of catechol *O*-methyltransferase (COMT) inhibitors and their therapeutic utility. *J. Med. Chem.* **2014,** *57*, 8692-8717.

16. Giles, R. E.; Miller, J. W. The catechol-O-methyl transferase activity and endogenous catecholamine content of various tissues in the rat and the effect of administration of U-0521 (3',4'-dihydroxy-2-methyl propiophenone). *J. Pharmacol. Exp. Ther.* **1967,** *158*, 189-194.

17. Assal, F.; Spahr, L.; Hadengue, A.; Rubbia-Brandt, L.; Burkhard, P. R. Tolcapone and fulminant hepatitis. *Lancet* **1998,** *352*, 958.

18. Parashos, S. A.; Wielinski, C. L.; Kern, J. A. Frequency, reasons, and risk factors of entacapone discontinuation in Parkinson disease. *Clin. Neuropharmacol.* **2004,** *27*, 119-123.

19. Almeida, L.; Rocha, J. F.; Falcao, A.; Palma, P. N.; Loureiro, A. I.; Pinto, R.; Bonifacio, M. J.; Wright, L. C.; Nunes, T.; Soares-da-Silva, P. Pharmacokinetics, pharmacodynamics and tolerability of opicapone, a novel catechol-O-methyltransferase inhibitor, in healthy subjects: prediction of slow enzyme-inhibitor complex dissociation of a short-living and very long-acting inhibitor. *Clin. Pharmacokinet.* **2013,** *52*, 139-151.

20. Rocha, J. F.; Almeida, L.; Falcao, A.; Palma, P. N.; Loureiro, A. I.; Pinto, R.; Bonifacio, M. J.; Wright, L. C.; Nunes, T.; Soares-da-Silva, P. Opicapone: a short lived and very long acting novel catechol-O-methyltransferase inhibitor following multiple dose administration in healthy subjects. *Br. J. Clin. Pharmacol.* **2013,** *76*, 763-775.

21. Ferreira, J. J.; Rocha, J. F.; Falcao, A.; Santos, A.; Pinto, R.; Nunes, T.; Soares-da-Silva, P. Effect of opicapone on levodopa pharmacokinetics, catechol-O-methyltransferase activity and motor fluctuations in patients with Parkinson's disease. *Eur. J. Neurol.* **2015,** *22*, 815-825, e56.

22. Robinson, R. G.; Smith, S. M.; Wolkenberg, S. E.; Kandebo, M.; Yao, L.; Gibson, C. R.; Harrison, S. T.; Polsky-Fisher, S.; Barrow, J. C.; Manley, P. J.; Mulhearn, J. J.; Nanda, K. K.; Schubert, J. W.; Trotter, B. W.; Zhao, Z.; Sanders, J. M.; Smith, R. F.; McLoughlin, D.; Sharma, S.; Hall, D. L.; Walker, T. L.; Kershner, J. L.; Bhandari, N.; Hutson, P. H.; Sachs, N. A. Characterization of non-nitrocatechol pan and isoform specific catechol-O-methyltransferase inhibitors and substrates. *ACS Chem. Neurosci.* **2012,** *3*, 129-140.

23. Harrison, S. T.; Poslusney, M. S.; Mulhearn, J. J.; Zhao, Z.; Kett, N. R.; Schubert, J. W.; Melamed, J. Y.; Allison, T. J.; Patel, S. B.; Sanders, J. M.; Sharma, S.; Smith, R. F.; Hall, D. L.; Robinson, R. G.; Sachs, N. A.; Hutson, P. H.; Wolkenberg, S. E.; Barrow, J. C. Synthesis and evaluation of heterocyclic catechol mimics as inhibitors of catechol-O-methyltransferase (COMT). *ACS Med. Chem. Lett.* **2015,** *6*, 318-323.

24. Zhao, Z.; Harrison, S.T.; Schubert J.W.; Sanders J.M.; Polsky-Fisher, S.; Zhang, N.R.; McLoughlin, D.; Gibson, C.R.; Robinson, R.G.; Sachs, N.A.; Kandebo, M.; Yao, L.; Smith, S.M.; Hutson, P.H.; Wolkenberg, S.E.; Barrow, J.C. Synthesis and optimization of N-heterocyclic pyridinones as catechol-O-methyltransferase (COMT) inhibitors. *Bioorg. Med. Chem. Lett.* **2016**, *26*, 2952–2956

25. Silva, T.; Oliveira, C.; Borges, F. Caffeic acid derivatives, analogs and applications: a patent review (2009 – 2013). *Expert Opin. Ther. Pat.* **2014,** *24*, 1257-1270.

26. Ardah, M. T.; Paleologou, K. E.; Lv, G.; Abul Khair, S. B.; Kazim, A. S.; Minhas, S. T.; Al-Tel, T. H.; Al-Hayani, A. A.; Haque, M. E.; Eliezer, D.; El-Agnaf, O. M. Structure activity relationship of phenolic acid inhibitors of alpha-synuclein fibril formation and toxicity. *Front. Aging Neurosci.* **2014,** *6*, 197.

27. dos Santos, N. A.; Martins, N. M.; Silva Rde, B.; Ferreira, R. S.; Sisti, F. M.; dos Santos, A. C. Caffeic acid phenethyl ester (CAPE) protects PC12 cells from MPP+ toxicity by inducing the expression of neuron-typical proteins. *Neurotoxicology* **2014,** *45*, 131-138.

28. Yis, U.; Topcu, Y.; Ozbal, S.; Tugyan, K.; Bayram, E.; Karakaya, P.; Yilmaz, O.; Kurul, S. H. Caffeic acid phenethyl ester prevents apoptotic cell death in the developing rat brain after pentylenetetrazole-induced status epilepticus. *Epilepsy Behav.* **2013,** *29*, 275-280.

29. Visioli, F.; De La Lastra, C. A.; Andres-Lacueva, C.; Aviram, M.; Calhau, C.; Cassano, A.; D'Archivio, M.; Faria, A.; Fave, G.; Fogliano, V.; Llorach, R.; Vitaglione, P.; Zoratti, M.; Edeas, M. Polyphenols and human health: a prospectus. *Crit. Rev. Food Sci. Nutr.* **2011,** *51*, 524-546.

30. Bäckström, R.; Honkanen, E.; Pippuri, A.; Kairisalo, P.; Pystynen, J.; Heinola, K.; Nissinen, E.; Linden, I.B.; Männistö, P.T.; Kaakkola. S.; Pohto P. Synthesis of some novel potent and selective catechol *O*-methyltransferase inhibitors. *J. Med. Chem.* **1989**, *32*, 841-846.

31. Karhunen, T.; Tilgmann, C.; Ulmanen, I.; Julkunen, I.; Panula, P. Distribution of catechol-O-methyltransferase enzyme in rat tissues. *J. Histochem. Cytochem.* **1994,** *42*, 1079-1090.

32. Lotta, T.; Vidgren, J.; Tilgmann, C.; Ulmanen, I.; Melen, K.; Julkunen, I.; Taskinen, J. Kinetics of human soluble and membrane-bound catechol O-methyltransferase: a revised mechanism and description of the thermolabile variant of the enzyme. *Biochemistry* **1995,** *34*, 4202-4210.

33. Huotari, M.; Gogos, J. A.; Karayiorgou, M.; Koponen, O.; Forsberg, M.; Raasmaja, A.; Hyttinen, J.; Mannisto, P. T. Brain catecholamine metabolism in catechol-O-methyltransferase (COMT)-deficient mice. *Eur. J. Neurosci.* **2002,** *15*, 246-256.

34. Roth, J. A. Membrane-bound catechol-O-methyltransferase: a reevaluation of its role in the O-methylation of the catecholamine neurotransmitters. *Rev. Physiol. Biochem. Pharmacol.* **1992,** *120*, 1-29.

35. Vieira-Coelho, M. A.; Soares-da-Silva, P. Effects of tolcapone upon soluble and membrane-bound brain and liver catechol-O-methyltransferase. *Brain Res.* **1999,** *821*, 69-78.

36. Bacq, Z. M.; Gosselin, L.; Dresse, A.; Renson, J. Inhibition of O-methyltransferase by catechol and sensitization to epinephrine. *Science* **1959,** *130*, 453-454.

37. Cardoso, F. L.; Brites, D.; Brito, M. A. Looking at the blood-brain barrier: molecular anatomy and possible investigation approaches. *Brain Res. Rev.* **2010,** *64*, 328-363.

38. van Asperen, J.; Mayer, U.; van Tellingen, O.; Beijnen, J. H. The functional role of P-glycoprotein in the blood-brain barrier. *J. Pharm. Sci.* **1997,** *86*, 881-884.

39. Di, L.; Kerns, E. H.; Fan, K.; McConnell, O. J.; Carter, G. T. High throughput artificial membrane permeability assay for blood-brain barrier. *Eur. J. Med. Chem.* **2003,** *38*, 223-232.

40. Crivori, P.; Cruciani, G.; Carrupt, P. A.; Testa, B. Predicting blood-brain barrier permeation from three-dimensional molecular structure. *J. Med. Chem.* **2000,** *43*, 2204-2216.

41. Zurcher, G.; Dingemanse J Fau - Da Prada, M.; Da Prada, M. Potent COMT inhibition by Ro 40-7592 in the periphery and in the brain. Preclinical and clinical findings. *Adv. Neurol*. **1993**, *60*, 641-647.

42. Zurcher, G.; Keller Hh Fau - Kettler, R.; Kettler R Fau - Borgulya, J.; Borgulya J Fau - Bonetti, E. P.; Bonetti Ep Fau - Eigenmann, R.; Eigenmann R Fau - Da Prada, M.; Da Prada, M. Ro 40-7592, a novel, very potent, and orally active inhibitor of catechol-O-methyltransferase: a pharmacological study in rats. *Adv. Neurol*. **1990**, *53*, 497-503

43. Silva, T.; Bravo, J.; Summavielle, T.; Remiao, F.; Perez, C.; Gil, C.; Martinez, A.; Borges, F. Biology-oriented development of novel lipophilic antioxidants with neuroprotective activity. *RSC Adv.* **2015,** 5, 15800-15811.

44. Hopkins, A. L.; Groom, C. R.; Alex, A. Ligand efficiency: a useful metric for lead selection. *Drug Discovery Today* **2004,** *9*, 430-431.

45. Keseru, G. M.; Makara, G. M. The influence of lead discovery strategies on the properties of drug candidates. *Nat. Rev. Drug Discovery* **2009,** *8*, 203-212.

46. Leeson, P. D.; Springthorpe, B. The influence of drug-like concepts on decision-making in medicinal chemistry. *Nat. Rev. Drug Discovery* **2007,** *6*, 881-890.

47. Lipinski, C. A.; Lombardo, F.; Dominy, B. W.; Feeney, P. J. Experimental and computational approaches to estimate solubility and permeability in drug discovery and development settings. *Adv. Drug Delivery Rev.* **2001,** *46*, 3-26.

48. Wager, T. T.; Hou, X.; Verhoest, P. R.; Villalobos, A. Moving beyond rules: the development of a central nervous system multiparameter optimization (CNS MPO) approach to enable alignment of druglike properties. *ACS Chem. Neurosci.* **2010,** *1*, 435-449.

49. Hitchcock, S. A.; Pennington, L. D. Structure−brain exposure relationships. *J. Med. Chem.* **2006,** *49*, 7559-7583.

50. Lobner, D. Comparison of the LDH and MTT assays for quantifying cell death: validity for neuronal apoptosis? *J. Neurosci. Methods* **2000,** *96*, 147-152.

51. Repetto, G.; del Peso, A.; Zurita, J. L. Neutral red uptake assay for the estimation of cell viability/cytotoxicity. *Nat. Protocols* **2008,** *3*, 1125-1131.

52. Haasio, K.; Koponen, A.; Penttila, K. E.; Nissinen, E. Effects of entacapone and tolcapone on mitochondrial membrane potential. *Eur. J. Pharmacol.* **2002,** *453*, 21-26.

53. Smith, K. S.; Smith, P. L.; Heady, T. N.; Trugman, J. M.; Harman, W. D.; Macdonald, T. L. In vitro metabolism of tolcapone to reactive intermediates: relevance to tolcapone liver toxicity. *Chem. Res. Toxicol.* **2003,** *16*, 123-128.

54. Naven, R. T.; Swiss, R.; Klug-McLeod, J.; Will, Y.; Greene, N. The development of structure-activity relationships for mitochondrial dysfunction: uncoupling of oxidative phosphorylation. *Toxicol. Sci.* **2013,** *131*, 271-278.

55. Gaspar, A.; Garrido, E. M.; Esteves, M.; Quezada, E.; Milhazes, N.; Garrido, J.; Borges, F. New insights into the antioxidant activity of hydroxycinnamic acids: Synthesis and physicochemical characterization of novel halogenated derivatives. *Eur. J. Med. Chem.* **2009,** *44*, 2092-2099.

56. Nematollahi, D. Kinetic study of 4-nitrocatechol oxidation using digital simulation of cyclic voltammograms. *J. Iran. Chem. Soc.* **2012,** 8, 803-810.

57. Panchompoo, J.; Aldous, L.; Compton, R. G. Size-effects in the chemical modification of carbon black nanoparticles with 4-nitroaniline. *New J. Chem.* **2010,** *34*, 2643-2653.

58. da Silva Julião, M. S.; Almeida, É. C.; La Scalea, M. A.; Ferreira, N. G.; Compton, R. G.; Serrano, S. H. P. Voltammetric behavior of nitrofurazone at highly boron doped diamond electrode. *Electroanalysis* **2005,** *17*, 269-274.

59. Squella, J.; Bollo, S.; Núñez-Vergara, L. Recent developments in the electrochemistry of some nitro compounds of biological significance. *Curr. Org. Chem.* **2005,** *9*, 565-581.

60. Galloway, S. M.; Vijayaraj Reddy, M.; McGettigan, K.; Gealy, R.; Bercu, J. Potentially mutagenic impurities: analysis of structural classes and carcinogenic potencies of chemical intermediates in pharmaceutical syntheses supports alternative methods to the default TTC for calculating safe levels of impurities. *Regul. Toxicol. Pharmacol.* **2013,** *66*, 326-335.

61. Chequer, F. M.; Lizier, T. M.; de Felicio, R.; Zanoni, M. V.; Debonsi, H. M.; Lopes, N. P.; de Oliveira, D. P. The azo dye Disperse Red 13 and its oxidation and reduction products showed mutagenic potential. *Toxicol. In Vitro* **2015,** *29*, 1906-1915.

62. Ben Mansour, H.; Corroler, D.; Barillier, D.; Ghedira, K.; Chekir, L.; Mosrati, R. Evaluation of genotoxicity and pro-oxidant effect of the azo dyes: acids yellow 17, violet 7 and orange 52, and of their degradation products by Pseudomonas putida mt-2. *Food Chem. Toxicol.* **2007,** *45*, 1670-1677.

63. Erikson, J. M.; Tweedie, D. J.; Ducore, J. M.; Prough, R. A. Cytotoxicity and DNA damage caused by the azoxy metabolites of procarbazine in L1210 tumor cells. *Cancer Res.***1989,** *49*, 127-133.

64. Vidgren, J.; Svensson, L. A.; Liljas, A. Crystal structure of catechol *O*-methyltransferase. *Nature* **1994,** *368*, 354-358.

65. Bonifacio, M. J.; Archer, M.; Rodrigues, M. L.; Matias, P. M.; Learmonth, D. A.; Carrondo, M. A.; Soares-Da-Silva, P. Kinetics and crystal structure of catechol-*O*-methyltransferase complex with co-substrate and a novel inhibitor with potential therapeutic application. *Mol. Pharmacol.* **2002,** *62,* 795-805.

66. Palma, P. N.; Rodrigues, M. L.; Archer, M.; Bonifacio, M. J.; Loureiro, A. I.; Learmonth, D. A.; Carrondo, M. A.; Soares-da-Silva, P. Comparative study of ortho- and meta-nitrated inhibitors of catechol-*O*-methyltransferase: interactions with the active site and regioselectivity of *O*-methylation. *Mol. Pharmacol.* **2006,** *70*, 143-153.

67. Liu, J.; Du, Y. Caffeic acid derivatives and their use in improving neuronal cell viability. Patent Id: WO2012068038 A2 **2012**.

68. Gaspar, A.; Silva, T.; Yanez, M.; Vina, D.; Orallo, F.; Ortuso, F.; Uriarte, E.; Alcaro, S.; Borges, F. Chromone, a privileged scaffold for the development of monoamine oxidase inhibitors. *J. Med. Chem.* **2011,** *54*, 5165-5173.

69. Pontes, H.; Sousa, C.; Silva, R.; Fernandes, E.; Carmo, H.; Remiao, F.; Carvalho, F.; Bastos, M. L. Synergistic toxicity of ethanol and MDMA towards primary cultured rat hepatocytes. *Toxicology* **2008,** *254*, 42-50.

Table of Contents Graphic

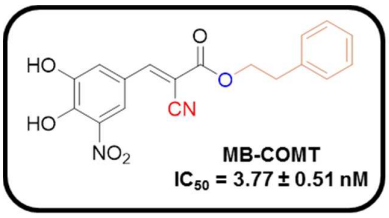

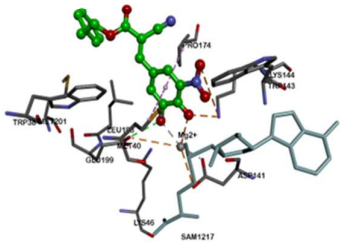

Table of Contents Graphic

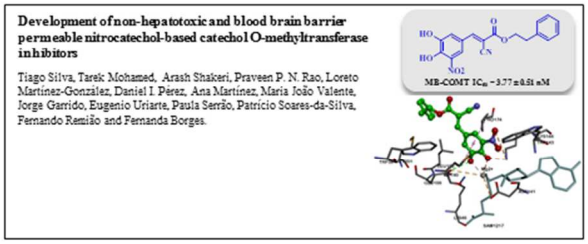

190x254mm (96 x 96 DPI)